

Article

Semisynthetic Sesquiterpene Lactones Generated by the Sensibility of Glaucolide B to Lewis and Brønsted–Lowry Acids and Bases: Cytotoxicity and Anti-Inflammatory Activities

Layzon A. Lemos da Silva ¹, Louis P. Sandjo ^{2,*} , Laura S. Assunção ¹, Anne N. Prigol ¹, Carolina D. de Siqueira ¹, Tânia B. Creczynski-Pasa ³, Marcus T. Scotti ⁴ , Luciana Scotti ⁴ , Fabíola B. Filippin-Monteiro ⁵ 
and Maique W. Biavatti ^{3,*}

¹ Post-Graduate Program of Pharmacy, Universidade Federal de Santa Catarina, Campus Universitário–Trindade, Florianópolis CEP 8840-970, SC, Brazil

² Department of Chemistry, Universidade Federal de Santa Catarina, Campus Universitário–Trindade, Florianópolis CEP 88040-900, SC, Brazil

³ Department of Pharmaceutical Sciences, Universidade Federal de Santa Catarina, Campus Universitário–Trindade, Florianópolis CEP 88040-970, SC, Brazil

⁴ Post-Graduate Program in Natural and Synthetic Bioactive Products, Universidade Federal da Paraíba, Cidade Universitária–Castelo Branco III, João Pessoa CEP 58051-900, PB, Brazil

⁵ Department of Clinical Analysis, Universidade Federal de Santa Catarina, Campus Universitário–Trindade, Florianópolis CEP 88040-900, SC, Brazil

* Correspondence: p.l.sandjo@ufsc.br (L.P.S.); maique.biavatti@ufsc.br (M.W.B.);
Tel.: +55-48-3721-3624 (L.P.S.); +55-48-3721-3493 (M.W.B.)



Citation: da Silva, L.A.L.; Sandjo, L.P.; Assunção, L.S.; Prigol, A.N.; de Siqueira, C.D.; Creczynski-Pasa, T.B.; Scotti, M.T.; Scotti, L.; Filippin-Monteiro, F.B.; Biavatti, M.W. Semisynthetic Sesquiterpene Lactones Generated by the Sensibility of Glaucolide B to Lewis and Brønsted–Lowry Acids and Bases: Cytotoxicity and Anti-Inflammatory Activities. *Molecules* **2023**, *28*, 1243. <https://doi.org/10.3390/molecules28031243>

Academic Editor: Arjun H. Banskota

Received: 26 December 2022

Revised: 16 January 2023

Accepted: 20 January 2023

Published: 27 January 2023



Copyright: © 2023 by the authors. Licensee MDPI, Basel, Switzerland. This article is an open access article distributed under the terms and conditions of the Creative Commons Attribution (CC BY) license (<https://creativecommons.org/licenses/by/4.0/>).

Abstract: Sesquiterpene lactone (SL) subtypes including hirsutinolide and cadinanolide have a controversial genesis. Metabolites of these classes are either described as natural products or as artifacts produced via the influence of solvents, chromatographic mobile phases, and adsorbents used in phytochemical studies. Based on this divergence, and to better understand the sensibility of these metabolites, different pH conditions were used to prepare semisynthetic SLs and evaluate the anti-inflammatory and antiproliferative activities. Therefore, glaucolide B (**1**) was treated with various Brønsted–Lowry and Lewis acids and bases—the same approach was applied to some of its derivatives—allowing us to obtain 14 semisynthetic SL derivatives, 10 of which are hereby reported for the first time. Hirsutinolide derivatives **7a** ($CC_{50} = 5.0 \mu\text{M}$; $SI = 2.5$) and **7b** ($CC_{50} = 11.2 \mu\text{M}$; $SI = 2.5$) and the germacranolide derivative **8a** ($CC_{50} = 3.1 \mu\text{M}$; $SI = 3.0$) revealed significant cytotoxic activity and selectivity against human melanoma SK-MEL-28 cells when compared with that against non-tumoral HUVEC cells. Additionally, compounds **7a** and **7c.1** showed strongly reduced interleukin-6 (IL-6) and nitrite (NOx) release in pre-treated M1 macrophages J774A.1 when stimulated with lipopolysaccharide. Despite the fact that hirsutinolide and cadinanolide SLs may be produced via plant metabolism, this study shows that acidic and alkaline extraction and solid-phase purification processes can promote their formation.

Keywords: sesquiterpene lactones; semisynthesis; anti-inflammatory activity; cytotoxic activity

1. Introduction

Glaucolide (Figure 1) is a germacranolide subtype of sesquiterpene lactones (SLs) commonly found in the Asteraceae family whose structure contains a C-7/C-11 endocyclic α,β -unsaturated γ -lactone ring [1]. Hirsutinolide (Figure 1) and cadinanolide structural isomers—vernojalcanolide and vernomargolide (Figure 1)—are also found in Asteraceae, especially in the Vernonieae tribe [2–4]. The genesis of hirsutinolide and cadinanolide remains unclear in the scientific literature. While some phytochemical studies performed on the Vernonieae species claimed that these skeletons are natural metabolites [5–7], others

reported that hirsutinolides and cadinanolides as presumable artifacts from the natural glaucolides produced during plant extraction and/or during the fractionation process [8–10]. Some previous studies carried out reactions mimicking the chromatographic purification of SLs, demonstrating that silica gel caused the conversion of glaucolide into hirsutinolide [11] and cadinanolide [12,13]. A similar goal was reached when various hirsutinolides and cadinanolides were obtained after treating glaucolide A in methanol (MeOH) or ethanol (EtOH) with alumina or silica gel [14]. Likewise, the acidic absorbent bentonite (composed of metallic oxides) was used to prepare 5 β -hydroxy-hirsutinolide from glaucolide B [15].

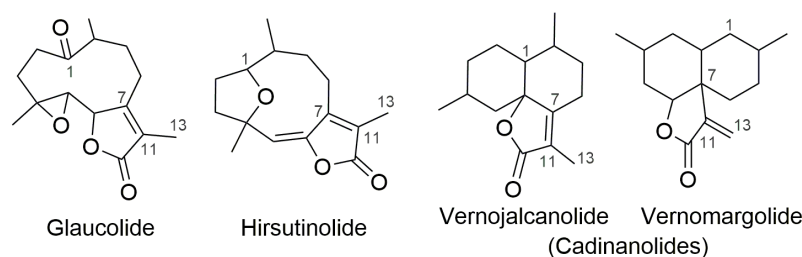


Figure 1. Carbocyclic skeletons of sesquiterpene lactone subtypes.

Analysis of isolation procedures reported in the literature for glaucolides and hirsutinolides revealed that the crude extracts were obtained via alcoholic maceration and were purified through successive silica gel chromatographic columns [10,16,17]. Although in some cases hirsutinolides were obtained solely [18–20], other phytochemical studies led to the identification of hirsutinolides, cadinanolides, and derivatives bearing methyl and ethyl ether functionalities [21–23]. These results suggest that protic solvents such as MeOH and EtOH as well as acid and alkaline stationary phases seem to contribute to glaucolide conversion, producing artifacts via addition, substitution, and annulation reactions during the purification process [21,24].

SLs are well-known as cytotoxic and antiproliferative agents for cancer cells [25–28]. Some hirsutinolides inhibited the growth of glioblastoma (U251MG and SF259) and breast cancer (MDA-MB-231) human tumor cell lines by affecting the activation and function of STAT3 [29]. This transcriptional factor activates the malignant state and controls the expression of target genes crucial for cell proliferation, also playing a key role in different aspects of the tumorigenic process in several cancers [30,31]. Moreover, 5 β -hydroxy-hirsutinolide induced apoptosis in MDA-MB-231, SK-LU-1 (lung cancer), and CaSki (cervical cancer, HPV 16 positive) cells by removing the anti-apoptotic Bcl-2 proteins from the cells and by increasing pro-apoptotic proteins Bax, active caspase-8, and active caspase-9 [15].

Among the different types of cancer, melanoma is considered the most aggressive skin cancer, and almost 290 thousand new cases were detected worldwide in 2018, causing about 60 thousand deaths [32]. The National Cancer Institute of Brazil [33] estimated about 1800 deaths in 2017 because of melanoma and suggested there will be almost 8500 new cases of melanoma (including 4200 men and 4250 women) per year between 2020 and 2022. SLs showed cytotoxic activity against different melanoma cell lines by inducing apoptosis cell death and affecting different pro-inflammatory, anti-apoptotic, and antioxidant intracellular mediators and signaling pathways [26,34,35]. Guaianolides, for example, were able to improve melanogenesis by increasing the melanin content and tyrosinase activity of B16 melanoma cells [36].

Based on the data presented above, this study was designed to explore the chemical transformation of glaucolide B in pH-dependent conditions using Brønsted–Lowry and Lewis acids and bases as catalysts. We herein report the preparation and structure elucidation of semisynthetic sesquiterpene lactones, as well as their *in vitro* anti-inflammatory potential and their antiproliferative activity in human melanoma SK-MEL-28 cancer cells.

2. Results and Discussion

2.1. Semisynthetic Modifications from Glaucolide B

The extraction process based on leaf washing with acetone was previously used to selectively obtain glaucolide B (**1**) from *Lepidaploa chamissonis* (Less.) H. Rob [37]. The obtained crude extract was purified using single-step centrifugal partition chromatography employing the M HEMWat (*n*-hexane/ethyl acetate/methanol/water, 5:6:5:6) biphasic solvent system [37]. The choice of this silica-gel-free purification technique aimed to avoid any degradation that could change the SL profile of *L. chamissonis*. As mentioned before, the silica gel stationary phase increases the possibility of structure modification of SLs during the chromatographic purification [14]. Glaucolide B (**1**) was subjected to various chemical modifications using different Lewis and Brønsted–Lowry acids (BiCl_3 , SOCl_2 , Ac_2O , and TFA; $\text{pK}_a -0.25$) and bases (DMAP, $\text{pK}_a 9.5$; K_2CO_3 , $\text{pK}_a 10.3$) to explore its chemical behavior. These catalysts were selected based on their different reactivity as it depends on their solubility in organic solvents, acidity, and basicity. Their reactivity also depends on potential acidic hydrogen atoms in different functionalities.

Figure 2 shows glaucolide B (**1**), first treated with *N,N*-dimethylaminopyridine (DMAP) in MeOH under reflux conditions, producing two known decaline products, identified as 13-*O*-methylvernojalcanolide-8-*O*-acetate [38] (**2**) and 1,4-dihydroxy-5,8,10,13-tetraacetylcadin-7(11)-en-6,12-olide [8] (**3**), with yields of 4.9% and 2.6%, respectively. As shown in the proposed mechanism (Figure 3), DMAP removed the γ -H of the butyrolactone ring, and the remaining pair of electrons rearranged, causing the elimination of the acetate ion at C-13 and the formation of an α -exomethylene γ -lactone derivative (**1.2**). The two nucleophilic species, MeOH and AcOH, underwent a 1,4-addition to the exomethylene of the derivative **1.4**, which rearranged, producing the vernojalcanolide derivatives **2** and **3**, respectively (Figure 3). The same condition was repeated using dichloromethane (CH_2Cl_2 , aprotic solvent) to reduce the chance of a side reaction with MeOH, and then, compound **3** was obtained with a yield of 30.3%. Similar vernojalcanolides bearing a methacryloyloxy group at C-8 instead of an acetoxy were previously obtained when glaucolide A was treated with silica gel in MeOH or EtOH [12,14].

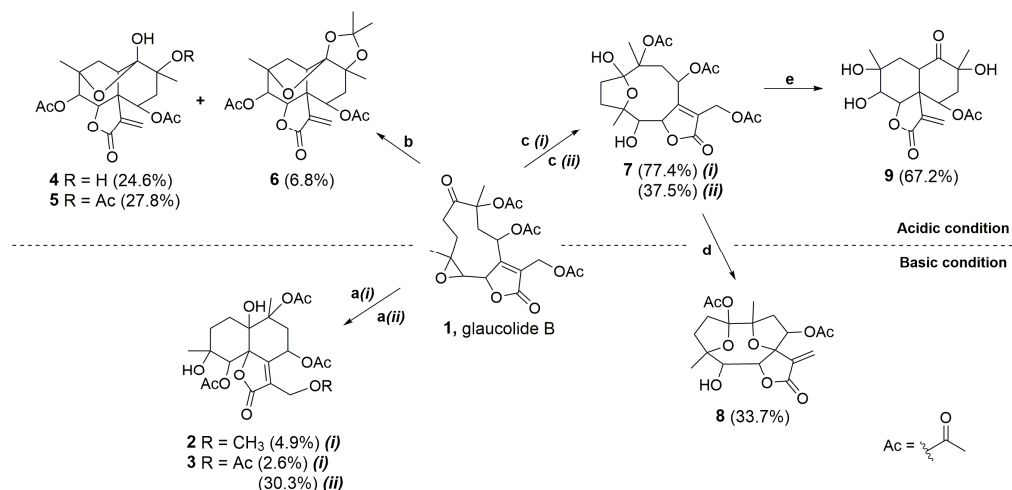


Figure 2. Acidic and basic conditions for the chemical transformation of glaucolide B (**1**). Reaction conditions: (a) (i) DMAP, MeOH, reflux at 60 °C, 3 h or (ii) DMAP, CH₂Cl₂, rt, 0.5 h; (b) BiCl₃, Ac₂O, CH₂Cl₂, Ar, rt, 2 h; (c) (i) BiCl₃, CH₂Cl₂, Ar, rt, 3 h or (ii) TFA-H₂O, CH₂Cl₂, -2 °C to rt, 24 h; (d) K₂CO₃ (aq.), THF, reflux at 45 °C, 2 h; and (e) BiCl₃, CH₂Cl₂, reflux at 50 °C, 15 h. Percentage of reaction yield in parentheses.

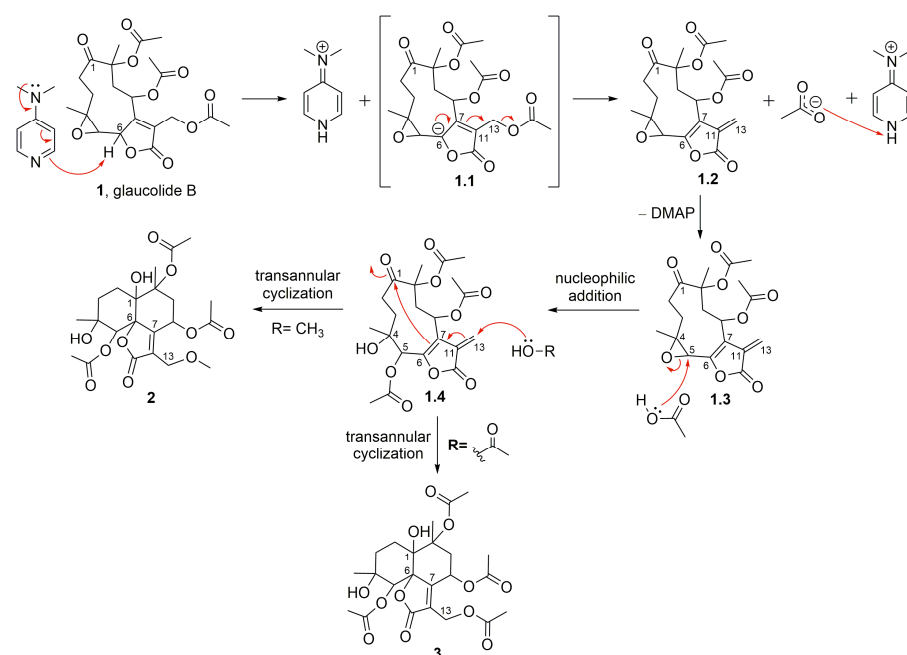


Figure 3. Proposed mechanism for the formation of semisynthetic derivatives **2** and **3** (red arrows illustrate the arrow-pushing mechanism).

Moreover, glaucolide B (**1**) transformation was explored under Lewis acidic conditions. From this reaction, three new acetalic vernomargolides were obtained and identified as 5,8-diacetoxy-2-*epi*-vernomargolide-1,4-cyclosemiacetal (**4**), 5,8,10-triacetoxy-2-*epi*-vernomargolide-1,4-cyclosemiacetal (**5**), and 5,8-diacetoxy-2-*epi*-vernomargolide-1,4-cycloacetal-1,10-acetonide (**6**). The formation of these compounds was possible by treating glaucolide B (**1**) with bismuth chloride (BiCl_3) and acetic anhydride (Ac_2O) in CH_2Cl_2 (Figure 2). The chemical profile of the obtained products indicated that the mixture of BiCl_3 and Ac_2O causes the formation of sub-products including a bismuth acetoxychloride [$\text{Bi}(\text{OAc})\text{Cl}_2$] species and acetone, as shown in Figure 4A, involved in the production of the acetalic vernomargolides **4**, **5**, and **6**. In an earlier study, BiCl_3 promoted the C-acetylation of trimethylsilyl enol ethers via acetyl chloride yielding β -diketones [39]. For vernomargolide derivatives, the epoxide at C-4/C-5 in glaucolide B (**1**) was opened via the nucleophilic addition at C-5 of the acetoxy [40] after complexation with $\text{Bi}(\text{OAc})\text{Cl}_2$, with the subsequent nucleophilic addition of the ketone to produce the anionic intermediate **1.5**. The resulting alkoxide of **1.5** performed a rearrangement via 1,3-hydrogen displacement, followed by annulation and allylic shift with $\text{Bi}(\text{OAc})\text{Cl}_2$ elimination (Figure 4B), producing compound **4**. Compound **5** was produced by eliminating bismuth hydroxy chloride [$\text{Bi}(\text{OH})\text{Cl}_2$] after the hydrolysis of the bismuth complex of the intermediate **4.2**—formed via complexation of the $\text{Bi}(\text{OAc})\text{Cl}_2$ with the C-10 tertiary ester in compound **4**—with the elimination of Ac_2O (Figure 4B). Products structurally related to **4** and **5** (presenting a methacryloyloxy group at C-8) were previously prepared from glaucolide A by using boron trifluoride [41]. Additionally, an unexpected acetalic product (compound **6**) was obtained, although acetone was used neither for the reaction nor as a mobile phase for chromatographic purification. Therefore, acetone might be formed via sequential reactions including hydrolysis, C-acetylation, and decarboxylation from the mixture of BiCl_3 and Ac_2O (Figure 4A). Such reactions of hydrolysis, decarboxylation, and acetalization promoted by BiCl_3 on carbonyl compounds were previously reported in [42–44]. Acetone was reacted via 1,2-addition with vicinal OH groups in **4.2** to produce a 2,2-dimethyl-1,3-dioxolane ring (compound **6**).

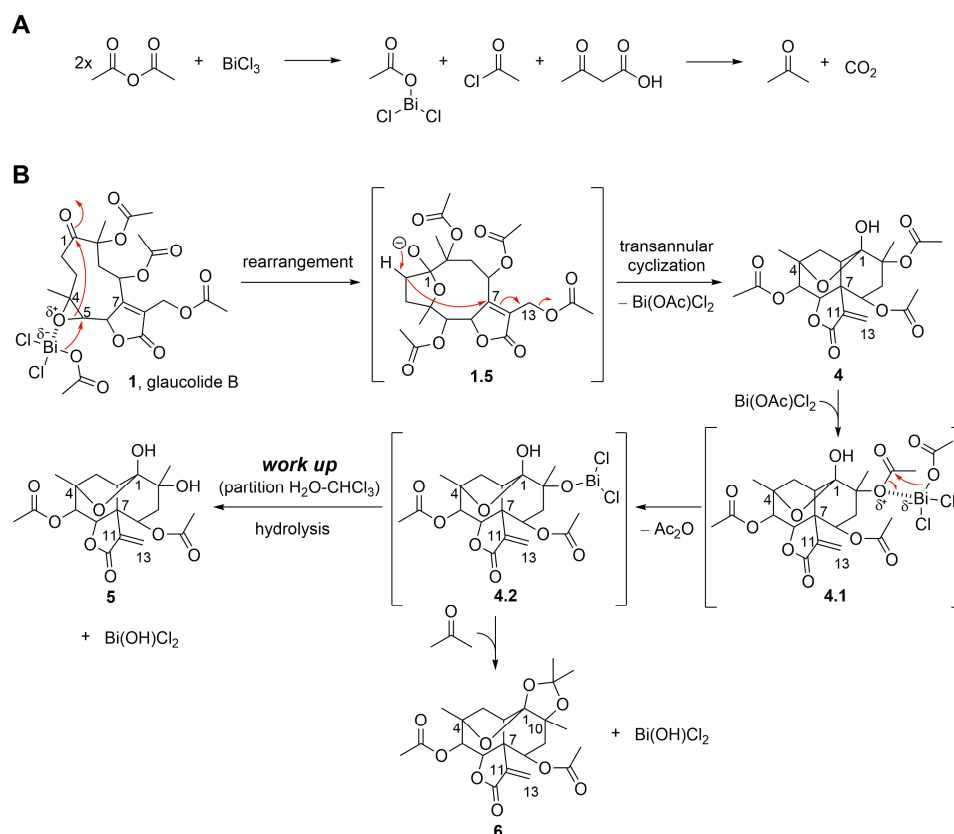


Figure 4. Proposed mechanism for the formation of SL semisynthetic derivatives 4–6 involving acetone formation (A) and SL-BiCl₃ complexation (B) (red arrows illustrate the arrow-pushing mechanism).

The importance of acetic anhydride for the conversion of gluacolide B (1) into cadinanolides was further explored by stirring 1 only with BiCl₃ in CH₂Cl₂. Instead of a cadinanolide, gluacolide B (1) was converted into a known hirsutinolide analog named 5-hydroxy-hirsutinolide [15] (7) with a yield of 77.4%. Its formation might involve the epoxy ring opening and cyclization (Figures 2 and 5) caused by bismuth(III) salt, as previously reported in [44,45]. The same hirsutinolide (7) was obtained with a lower yield (37.5%) when gluacolide B (1) was stirred together with trifluoroacetic acid (TFA) (Figure 2). While the alkaline conditions (use of DMAP) and the use of BiCl₃/Ac₂O caused the conversion of gluacolide into decaline scaffolds, reactions using Lewis and Brønsted–Lowry acids solely favored a rearrangement of gluacolide into the hirsutinolide analog.

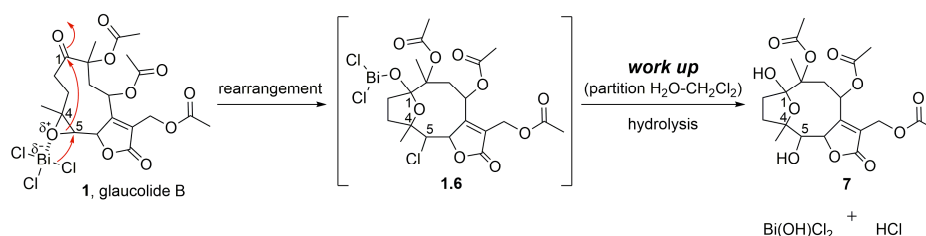


Figure 5. Proposed mechanism for the formation of SL semisynthetic derivative 7 (red arrows illustrate the arrow-pushing mechanism).

Calculation of the electronic energies revealed that compound 7 was formed from gluacolide B (1) with a difference of enthalpy of -77.3527 kcal/mol (Figure 6). The energy proximity of both compounds suggests why phytochemical adsorbents such as silica gel, Florisil, and alumina convert gluacolide into hirsutinolide derivatives during the separation

process. The energetic barrier for the chemical conversion suggests that the stability of a glaucolide-type might depend on the pH of the plant crude extract in the solvent. The preparation condition of this conversion indicates that hirsutinolide derivatives might be formed kinetically from glaucolides.

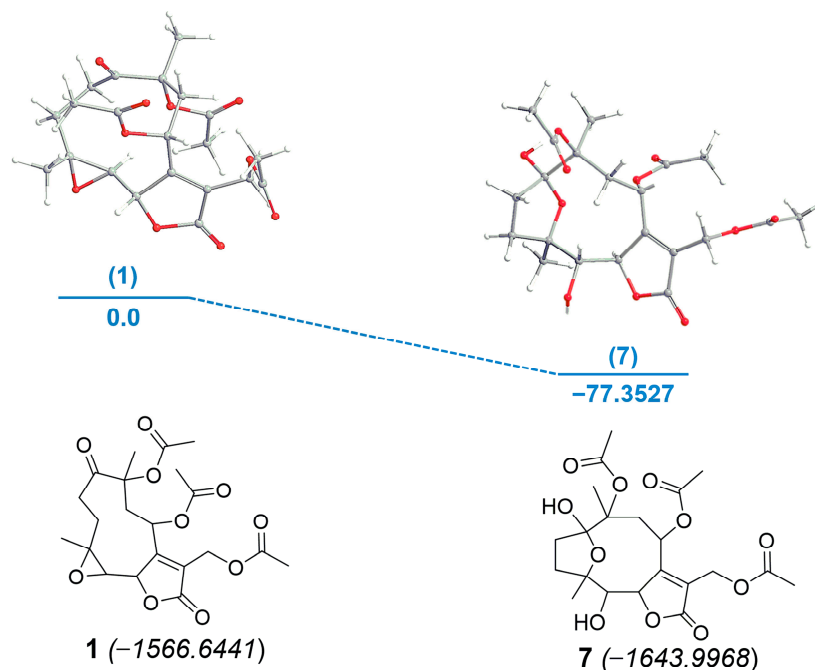


Figure 6. Energy diagram for the formation of SL semisynthetic derivative 7 from 1. Relative energies [kcal/mol, B3LYP/6-31G*] (blue). Electronic energy values (italic) for compounds 1 and 7 are expressed in kcal/mol. Oxygens are represented as red atoms.

The semisynthetic product, compound 7, was further submitted to chemical modifications to investigate the influence of alkaline and acidic conditions (Figure 7). Thus, hirsutinolide analog 7 treated in alkaline conditions (Figure 8) using potassium carbonate (K_2CO_3) produced a new spiro(tetrahydrofuran- γ -butyrolactone) derivative identified as 1,8-diacetoxy-1(4),7(10)-diepoxy-5-hydroxygermacr-11(13)-en-6(12)-olide (8, 33.7%). The formation of 8 seems to be promoted by the deprotonation of the hemiacetalic hydroxyl moiety at C-1 due to the alkaline pH (Figure 8A). The alkoxide intermediate (7.1), after transesterification of the C-10 acetoxy, rearranged via annulation with a nucleophilic addition at C-7 and allylic shift, eliminated the C-13 acetoxy group as potassium acetate (CH_3COOK) and converted C-7 to a spiro carbon, producing an exocyclic methylene at C-11/C-13 (Figure 8B). Similar to derivative 8, SLs (bearing a π -bond at C5/C-6 instead of a hydroxymethyne at C-5) were produced from glaucolide and hirsutinolide by using K_2CO_3 under reflux in dioxane [38,46]. In addition, a related compound was also obtained via the silica gel chromatographic purification of a *Vernonia chamaedrys* crude extract [46].

Compound 7 also furnished a new vernomargolide analog, identified as 8-acetoxy-vernemargolide (9, 67.2%), when treated with the Lewis acid $BiCl_3$ under reflux in CH_2Cl_2 (Figure 7). As proposed in Figure 9, the mechanistic pathway for the formation of compound 9 included a rearrangement from hirsutinolide 7 to produce the tautomer ketone glaucolide intermediate 7.2, under reflux. After $BiCl_3$ complexation and the H- α elimination under the Lewis acid's influence, transannular cyclization occurred via the attack of C- α on the C- β of the lactone ring to furnish the vernomargolide intermediate (7.3). Regioselective hydrolysis of the bismuth complex at C-10 occurred via the intermediate 7.3 to produce compound 9 after eliminating the ketone α -acetoxy moiety. To the best of our knowledge, this is the first time that vernomargolide 9 was produced from a hirsutinolide, although being previously described in the silica gel chromatographic purification of *Vernonia marginata* in [5].

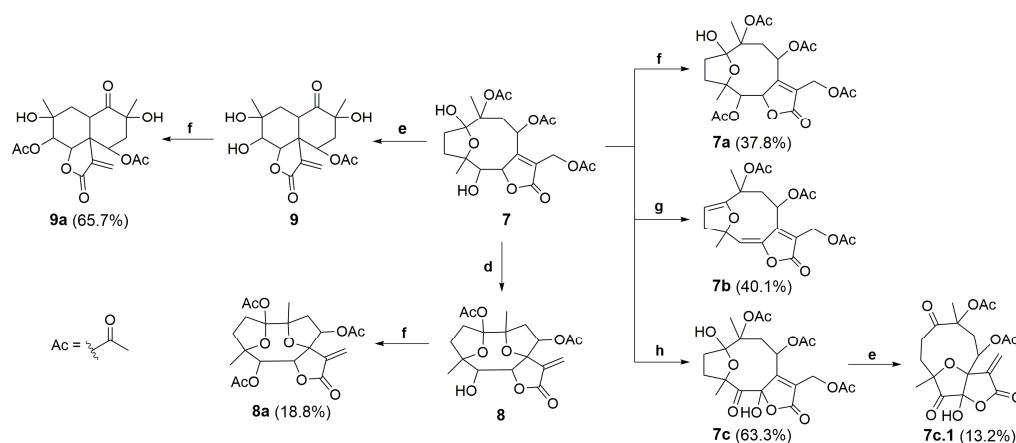


Figure 7. Conditions for the chemical transformations of compounds 7a–9a. Reaction conditions: (d) K_2CO_3 (aq.), THF, reflux at 45 °C, 2 h; (e) $BiCl_3$, CH_2Cl_2 , reflux at 50 °C, 15 h; (f) DMAP, Et_3N , Ac_2O , CH_2Cl_2 , $-10\text{ }^\circ\text{C}$, 0.5 h; (g) $SOCl_2$, pyridine, Ar, CH_2Cl_2 , $-10\text{ }^\circ\text{C}$ (0.5 h) to reflux at 60 °C (3.5 h); and (h) PCC/ SiO_2 (1:1), CH_2Cl_2 , Ar, rt, 48 h. Percentage of reaction yield in parentheses.

A



B

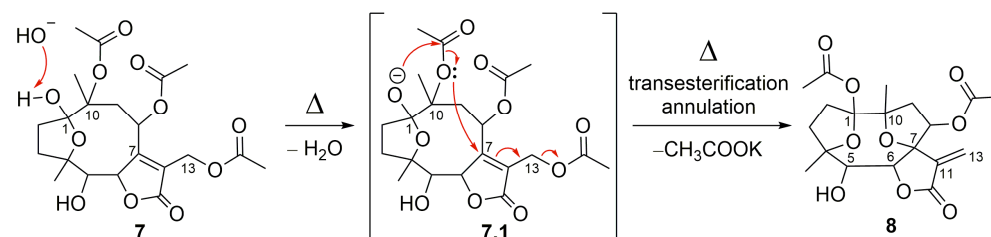


Figure 8. Proposed mechanism for the formation of SL semisynthetic derivative 8 involving an alkaline pH promoted by aqueous K_2CO_3 dissociation (A) and a rearrangement via transesterification and annulation (B) (red arrows illustrate the arrow-pushing mechanism).

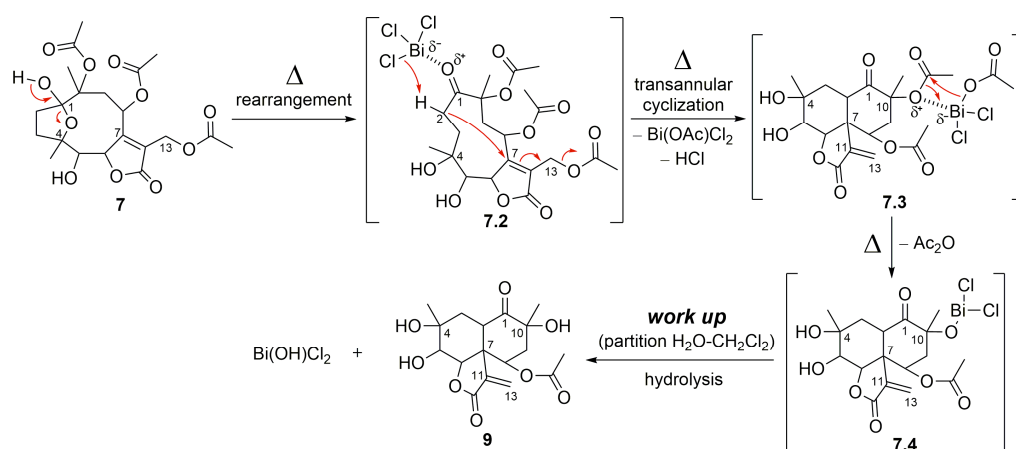


Figure 9. Proposed mechanism for the formation of SL semisynthetic derivative 9 (red arrows illustrate the arrow-pushing mechanism).

Compounds 7–9 were subjected to acetylation using Ac_2O with triethylamine (Et_3N) and DMAP in CH_2Cl_2 (Figure 7) via the alcohol acylation mechanism [47,48], producing

three new acetylated analogs, characterized as 5-acetoxy-hirsutinolide (**7a**, 37.8%), 1,5,8-triacetoxy-1(4),7(10)-diepoxy-germacr-11(13)-en-6(12)-olide (**8a**, 18.8%), and 5,8-diacetoxy-vernomargolide (**9a**, 65.7%), respectively. The acetylation occurred regioselectively in vernomargolide **9a** since the only secondary OH group in compound **9** was esterified. The two tertiary OHs at C-4 and C-10 remained free as in the starting material (**9**), presumably because of the neighboring steric effect promoted by the geminal methyl groups [49].

Compound **7** was also treated with thionyl chloride (SOCl₂) in pyridine to substitute OH functions (Figure 7). No chlorinated products were found, but a known product of elimination was obtained with a 40.1% yield, which was characterized as 8,10,13-triacetoxy-1(4)-epoxy-germacra-1(2),5(6),7(11)-trien-6(12)-olide (**7b**). The olefin functions observed in **7b** indicated the occurrence of double dehydrohalogenation [50] via chlorination at C-1 and C-5 of 5-hydroxy-hirsutinolide (**7**). Compound **7b** was previously reported in the literature and was produced from a hirsutinolide-type SL [51,52].

Moreover, after treating hirsutinolide **7** with pyridinium chlorochromate (PCC) fixed on silica gel (1:1, *w/w*), instead of a mono-oxidized product at C-5, a new product with two oxidized carbons bearing a 5-oxo-6-hydroxy- γ -lactone was obtained (Figure 7). Diagnostic spectroscopic data led to the structure of 8,10,13-triacetoxy-1(4)-epoxy-6-hydroxy-5-oxo-germacr-7(11)-en-6(12)-olide (**7c**). It seems that, besides the oxidation of the hydroxyl at C-5, the lactone ring opening in the presence of silica gel (7.5) formed the OH group attached to γ -C (7.8), which was oxidized also by PCC to yield a 5,6-diketone derivative (7.10). This diketone intermediate **7.10** further reacted with the carboxylic acid to produce the 5-oxo-6-hydroxy- γ -lactone derivative (**7c**), as proposed in the mechanism illustrated in Figure 10.

As illustrated in Figures 7 and 11, the oxidized hirsutinolide analog (**7c**) was further treated with BiCl₃ in reflux, aiming to prepare a vernomargolide derivative. Unexpectedly, a new 1,5-oxo-4(7)-epoxy-6-hydroxy- γ -butyrolactone derivative bearing a macrocyclic hydrocarbon ring was obtained (13.2%). Its structure was assigned as 8,10-diacetoxy-4(7)-epoxy-6-hydroxy-1,5-oxo-germacr-11(13)-en-6(12)-olide (**7c.1**) based on its spectrometric data. The proposed mechanism pathway to form **7c.1** (Figure 11) involved a tandem reaction process including hydrolysis of the C-1 hemiacetal ring after bismuth complexation under reflux and a nucleophilic attack at C-7, causing the allylic elimination of Bi(OAc)Cl₂. Although an oxidized decaline core was aimed to be the main product based on the preparation of compound **9** from the hirsutinolide **7**, the geometry of the oxidized carbons in the **7c** hydrocarbon macrocycle might disfavor the proximity between the C-2 and the α,β -unsaturation of the butyrolactone for the expected C-C bond formation, especially when compared with the presumably more favorable C-4/C-7 epoxy bridge rearrangement.

The structures of the prepared SLs were elucidated based on the spectroscopic data, including 1D and 2D nuclear magnetic resonance (NMR) and high-resolution mass spectrometry (HRESIMS) analyses (see the Experimental Section and Supplementary Materials for more details). The spectroscopic data of known compounds were also compared with those reported in the literature.

2.2. Biological Activity

Glucolide B (**1**) and its prepared derivatives were first evaluated for cytotoxic activities against three tumor cell lines including human melanoma (SK-MEL-28), human large-cell lung carcinoma (NCI-H460), and human glioblastoma cancer (SF295) cells, comparing with non-tumoral human umbilical vein endothelial cells (HUVECs) to determine the selectivity index (SI). As depicted in Table 1, hirsutinolides **7a** and **7b**, as well as germacranolide **8a**, showed significant cytotoxic activity and selectivity against human melanoma SK-MEL-28 cells, with CC₅₀ values of 5.0 μ M (SI = 2.5), 11.2 μ M (SI = 2.5), and 3.1 μ M (SI = 3.0), respectively. In addition, none of the evaluated compounds were active against cell lines NCI-H460 and SF295. Sesquiterpene lactones represent an important natural core for medicinal chemistry. The lactone ring and the α -methylene of SLs are two chemical features that can undergo 1,2- and 1,4-additions (Michael additions) to thiol-containing

proteins [53], conferring on SLs numerous biological activities including antitumor and anti-inflammatory activities. SLs bearing this α -methylene- γ -lactone moiety exert anti-tumor effects by modifying the redox balance in cells and/or by inhibiting the signaling pathway of nuclear factor kappa B (NF- κ B) [53]. NF- κ B is known to be an anti-apoptotic metastasis promoter and is involved in the immune system response, mainly responsible for orchestrating the production of inflammatory cytokines and cell proliferation [54]. Interestingly, parthenolide, a germacranolide-type SL, has been reported to trigger apoptosis also in human melanoma SK-MEL-28 cells by activating a caspase-independent mechanism mediated by the nuclear translocation of apoptosis inducing factor, which is associated with several events such as reactive oxygen species generation, the depletion of protein thiols and glutathione, and the dissipation of the mitochondrial membrane potential [55]. Likewise, the SLs tomentosin and inuviscolide presented antiproliferative activity against human melanoma SK-MEL-28 cells by inducing G₂/M arrest and apoptosis, whose mechanism was associated with a decrease in the mitochondrial membrane potential, caspase-3 activation, upregulations of p53 and p21 and down-regulation of the p65 subunit of NF- κ B, and surviving [35].

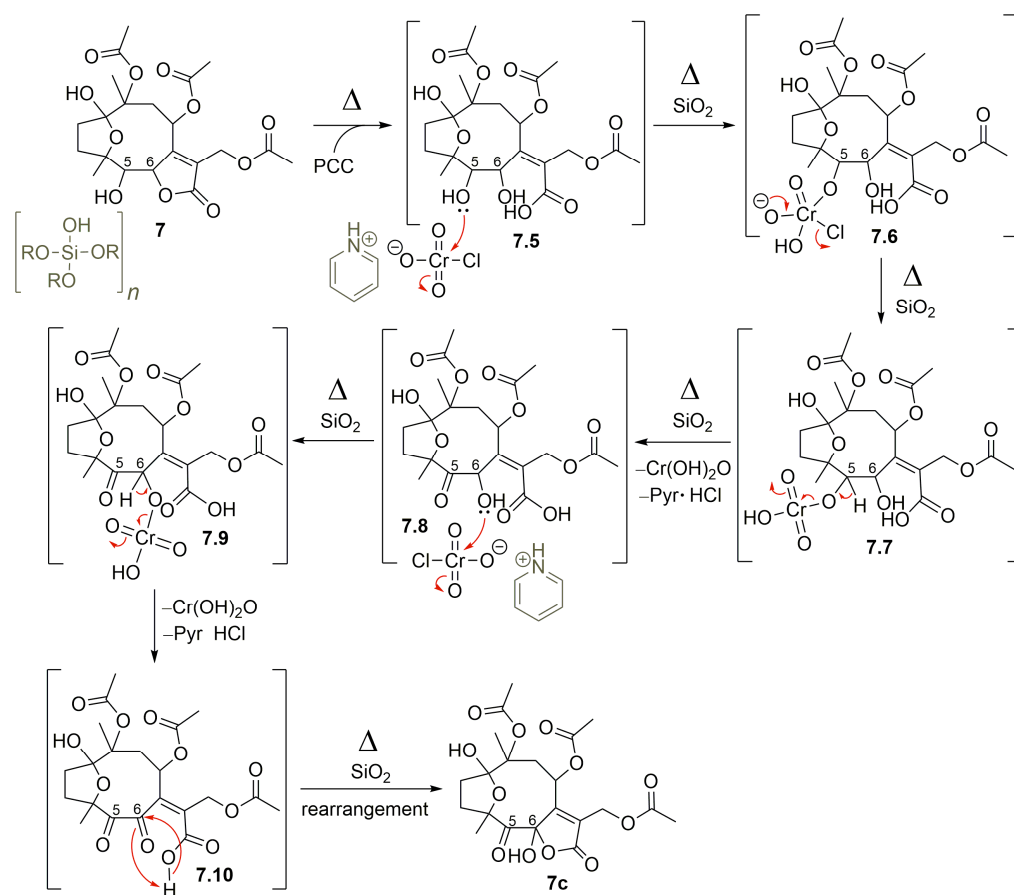


Figure 10. Proposed mechanism for the formation of SL semisynthetic derivative 7c (red arrows illustrate the arrow-pushing mechanism).

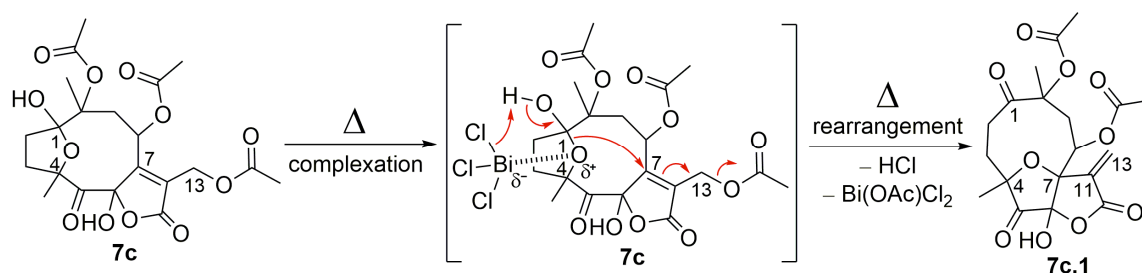


Figure 11. The proposed mechanism for the formation of SL semisynthetic derivative **7c.1** (red arrows illustrate the arrow-pushing mechanism).

Table 1. Viability, CC_{50} , and selectivity index (SI) values for the cytotoxic activity of the sesquiterpene lactones and semisynthetic derivatives.

Compound	Cell Lines							
	SK-MEL-28		SI	HUVEC	NCI-H460		SF295	
	Viability (%) ^a	CC_{50} (μ M)		CC_{50} (μ M)	Viability (%) ^a	CC_{50} (μ M)	Viability (%) ^a	CC_{50} (μ M)
Glaucolide B (1)	82.6 ± 4.1	n.d.	-	n.d.	85.1 ± 4.6	n.d.	88.0 ± 4.8	n.d.
Vernojalcanolide derivative (2)	87.1 ± 2.6	n.d.	-	n.d.	91.8 ± 3.6	n.d.	86.8 ± 6.3	n.d.
Vernojalcanolide derivative (3)	91.1 ± 1.7	n.d.	-	n.d.	88.4 ± 3.4	n.d.	86.1 ± 2.3	n.d.
Vernomargolide derivative (4)	96.4 ± 6.9	n.d.	-	n.d.	100.2 ± 2.7	n.d.	94.7 ± 1.1	n.d.
Vernomargolide derivative (5)	95.3 ± 4.1	n.d.	-	n.d.	100.3 ± 5.5	n.d.	95.6 ± 3.9	n.d.
Vernomargolide derivative (6)	85.9 ± 4.0	n.d.	-	n.d.	90.4 ± 1.5	n.d.	90.4 ± 3.7	n.d.
Hirsutinolide derivative (7)	76.2 ± 7.5	n.d.	-	n.d.	89.1 ± 3.9	n.d.	86.7 ± 3.8	n.d.
Hirsutinolide derivative (7a)	17.1 ± 3.3	5.0	2.5	12.7	74.6 ± 1.3	n.d.	86.9 ± 4.3	n.d.
Hirsutinolide derivative (7b)	16.0 ± 2.6	11.2	2.5	27.8	73.2 ± 1.0	n.d.	83.3 ± 1.2	n.d.
Hirsutinolide derivative (7c)	79.2 ± 6.4	n.d.	-	n.d.	85.7 ± 1.6	n.d.	88.6 ± 4.8	n.d.
Germacranolide derivative (7c.1)	77.3 ± 0.3	n.d.	-	n.d.	88.7 ± 6.7	n.d.	87.0 ± 4.7	n.d.
Germacranolide derivative (8)	66.9 ± 3.5	n.d.	-	n.d.	87.3 ± 1.6	n.d.	82.0 ± 4.7	n.d.
Germacranolide derivative (8a)	5.3 ± 0.3	3.1	3.0	9.0	53.1 ± 0.0	n.d.	67.3 ± 4.0	n.d.
Vernomargolide derivative (9)	74.5 ± 4.9	n.d.	-	n.d.	84.9 ± 0.4	n.d.	85.2 ± 2.8	n.d.
Vernomargolide derivative (9a)	73.8 ± 3.1	n.d.	-	n.d.	84.8 ± 0.9	n.d.	85.9 ± 5.0	n.d.
Piptocarphin A (10)	23.1 ± 4.2	6.7	1.9	12.5	104.8 ± 1.6	n.d.	93.2 ± 3.2	n.d.
Glaucolide A (11)	56.3 ± 1.4	14.6	1.4	20.4	95.1 ± 4.6	n.d.	91.8 ± 3.3	n.d.
Diacetylpiptocarphol (12)	9.0 ± 0.5	3.8	3.3	12.6	63.8 ± 6.9	n.d.	80.4 ± 3.3	n.d.

^a Results expressed as means ± standard deviation (n = 3); **n.d.**—not determined.

Although compounds **7a** and **8a** are not analogous, the increase in lipophilicity via acetylation (Figure 7) seems to have a beneficial effect on cytotoxic activity. These findings suggest a positive influence on the cytotoxic activity against SK-MEL-28 cells provided by the incorporation of an acetoxy substituent in the C-5 position of both compounds in comparison with the respective starting materials containing a hydroxyl function in the same position. The hirsutinolide skeleton and its polyoxygenated functionalities provides these products with biological potentials more than their respective analog starting materials. Moreover, the change in physical properties such as lipophilicity due to new acetoxy groups in compounds **7a** and **8a** appears to improve their cell absorption, subsequently leading to the observed biological effect [56–59]. Compound **7b** was also more lipophilic than its starting material (**7**), and, interestingly, it also showed cytotoxicity even though it was two-fold less than **7a**.

To better understand the influence of increased lipophilicity, three other SLs previously purified from Vernoniae species [60], namely, piptocarphin A (**10**), glaucolide A (**11**), and diacetylpiptocarphol (**12**) (Figure 12), were also evaluated for cytotoxicity properties against the same tumoral cell lines (Table 1). Although presenting a hydroxyl group at C-10 besides the lipophilic olefin function at C-5/C-6, when compared with hirsutinolide **7**, its congeners (**10** and **12**) were also promisingly active ($CC_{50} = 6.7 \mu\text{M}$; $SI = 1.9$ and $CC_{50} = 3.8 \mu\text{M}$; $SI = 3.3$, respectively) against SK-MEL-28 cells.

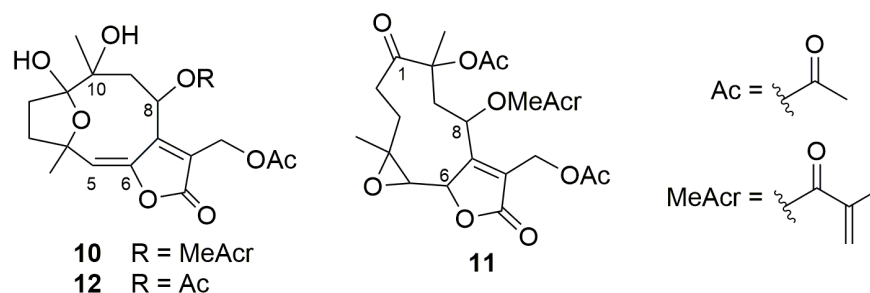


Figure 12. Structures of sesquiterpene lactones **10–12**.

The assessment of the anti-inflammatory activity of SL derivatives revealed that all compounds were anti-inflammatory to some degree (Figure 13). Pro-inflammatory M1-phenotype macrophages were used, via stimulation with lipopolysaccharide (LPS) through toll-like receptor 4 (TLR4), leading to the activation of the canonical NF- κ B pathway [61]. Such triggering leads to the activation of MyD88-dependent TLR signaling, which is crucial for the expression of NF- κ B, the key transcription factor of M1-macrophages and required for the induction of a large number of inflammatory genes, including those encoding IL-6 and NO [62]. Compounds **7a** and **7c.1** displayed a strong capacity to prevent NO $_x$ and IL-6 release from pre-treated M1-macrophages compared with control M1 cells (LPS + group) (approximately a 77% reduction, as shown in Figure 13A,B). Moreover, these compounds not only showed anti-inflammatory properties but also presented less cytotoxicity against macrophages (Figure S70, found in the Supplementary Materials). A similar profile is registered in previous reports [16,22,63] for the well-known compounds (**10** and **11**). Even though antitumor and anti-inflammatory signaling may interact with each other, herein, we observed the potential for all compounds to disturb NO and IL-6 production and release, affecting not only the exacerbated inflammatory response but also cell proliferation [64].

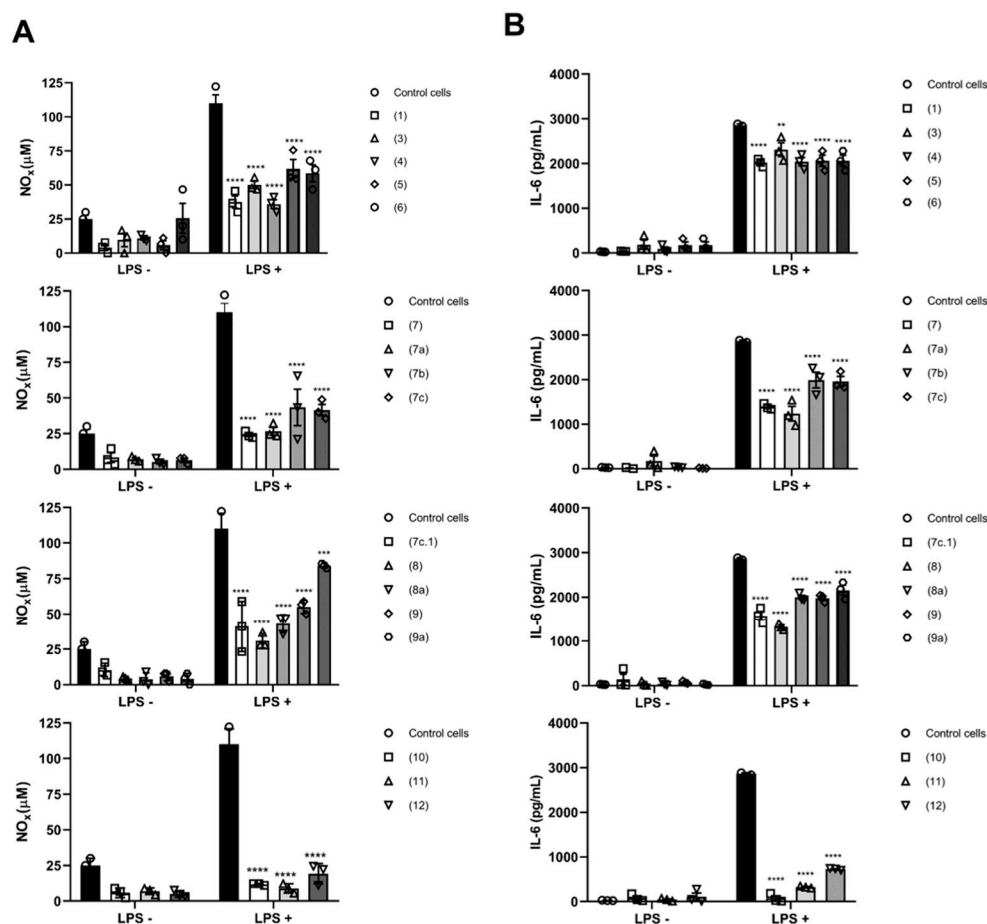


Figure 13. Anti-inflammatory activity evaluated from activated macrophages. (A) Total nitrite nitrate (NO_x) determination and (B) Interleukin 6 (IL-6) in the supernatants of control and LPS-stimulated macrophages (10 µg/mL) in the presence of CC₁₀ of compounds **1**, **3**, **4**, **5**, **7**, **7a**, **7b**, **7c**, **7c.1**, **8**, **8a**, **9**, **9a**, **10**, **11**, and **12**. Data expressed as means ± standard deviation of three independent experiments. A two-way analysis of variance followed by Sidak's multiple comparisons test was performed. ** $p < 0.01$, *** $p < 0.001$ and **** $p < 0.0001$ compared with control group LPS-not stimulated (LPS-) or LPS-stimulated (LPS+). Compound **2** was not evaluated.

3. Materials and Methods

3.1. General Experimental Procedures

UV spectra were recorded with a PDA detector from a Waters *Acquity UPLC H-class* system (Waters Co., Milford, MS, USA), and data were processed with *MassLynx 4.1* software. One-dimensional and two-dimensional NMR spectra were recorded with a Bruker *Fourier 300* spectrometer (Bruker Co., Billerica, MS, USA) using CDCl₃ (Cambridge Isotope Laboratories, Inc., Andover, MS, USA) as a solvent, and data were processed with *TopSpin 3.2* software. NMR chemical shifts were referenced to tetramethylsilane (TMS). LC-HRESIMS spectra were measured with a Waters *Xevo G2-S QToF* mass spectrometer (Waters Co., Manchester, UK) equipped with a ZsprayTM electrospray ionization probe and a quadrupole-time of flight (QToF) analyzer, coupled to a Waters *Acquity UPLC H-class* system, using a Thermo Scientific[®] *Hypersil GOLD* (100 × 3 mm, 1.9 µm) C₁₈ column and a 0.5 mL/min elution of a gradient system combining 0.1% aqueous formic acid and acetonitrile. Acetonitrile HPLC grade (Tedia[®] Brazil, Rio de Janeiro, Brazil), formic acid 85% *p.a.* grade (Vetec[®] Química Fina, Rio de Janeiro, Brazil), and ultrapure reverse osmosis Milli-Q water (prepared using a Millipore[®] Simplicity UV System from Millipore, France) were used for the eluent in the LC-MS analyses, while data were processed with *MassLynx 4.1* software. Column chromatography (CC) separations and solid-phase extraction (SPE)

were performed using silica gel 60 (240–400 mesh from SiliCycle[®], Quebec, QU, Canada) as support, and *p.a.* grade solvents, including *n*-hexane, dichloromethane (CH₂Cl₂), chloroform (CHCl₃), and acetone (Vetec[®] Química Fina, Rio de Janeiro, RJ, Brazil). Analytical and preparative TLC was carried out on silica gel 60 F₂₅₄ precoated aluminum plates (SiliCycle[®]). Spots were observed under UV (254 and 366 nm) light and reacted with anisaldehyde-sulfuric acid [65] for analytical TLC, while for preparative TLC, spots were monitored under UV light, collected, and filtered through G3 sintered glass with acetone.

3.2. Semisynthetic Derivatives Production and Isolation

Glaucolide B (**1**), a pale yellow amorphous solid used as a starting material for SL semisynthetic derivatives production, was previously obtained from a *Lepidaploa chamissonis* (Less.) H. Rob. extract after centrifugal partition chromatographic isolation [37]. To investigate glaucolide B transformation as well as its derivatives under the influence of different acidic and basic conditions, catalysts with varied acid–base properties were used in transannular via allylic rearrangement cyclization reactions, in addition to oxidation, dehydrohalogenation, acetylation, and elimination reactions.

For the semisynthesis of 13-*O*-methylvernojalcanolide-8-*O*-acetate (**2**) and 1,4-dihydroxy-5,8,10,13-tetraacetylcadin-7(11)-en-6,12-olide (**3**), condition *a(i)*, DMAP (1.5 mg, 0.01 mmol, 0.2 molar eq.) was added to a solution of glaucolide B (**1**; 30.1 mg, 0.07 mmol, 1 molar eq.) in MeOH (1 mL), and the mixture was refluxed at 60 °C for 3 h. TLC was used to monitor the reaction, which was stopped after the complete consumption of glaucolide B (**1**). The reaction mixture was concentrated under reduced pressure. The crude material was purified via silica gel CC using a gradient eluent system composed of acetone in *n*-hexane (20–50%, *v/v*) to obtain semisynthetic derivatives **2** (1.6 mg, 4.9%) and **3** (1.1 mg, 2.6%). Compound **2** was a yellowish amorphous solid; LC-UV [acetonitrile in 0.1% aqueous formic acid] λ_{max} 234 nm; ¹H NMR (CDCl₃, 300 MHz, at 295 K): δ 5.93 (1H, s, H-5), 5.87 (1H, dd, *J* = 4.0, 2.4 Hz, H-8), 4.42 (1H, d, *J* = 12.1 Hz, H-13a), 4.23 (1H, d, *J* = 12.1 Hz, H-13b), 3.35 (3H, s, OCH₃-13), 3.32 (1H, dd, *J* = 16.0, 2.4 Hz, H-9a), 2.42–2.33 (1H, m, H-2a), 2.37–2.26 (1H, m, H-3a), 2.22 (3H, s, OCOCH₃-10), 2.04 (1H, dd, *J* = 16.0, 4.0 Hz, H-9b), 2.04 (3H, s, OCOCH₃-8), 1.98 (3H, s, OCOCH₃-5), 1.92–1.81 (1H, m, H-3b), 1.73–1.66 (1H, m, H-2b), 1.70 (3H, s, CH₃-14), and 1.41 (3H, s, CH₃-15); ¹³C NMR (CDCl₃, 75 MHz, at 295 K): δ 171.4 (CO, C-12), 171.4 (CO, OCOCH₃-5), 170.5 (CO, OCOCH₃-8), 168.9 (CO, OCOCH₃-10), 157.2 (C, C-7), 129.5 (C, C-11), 88.9 (C, C-6), 84.2 (C, C-10), 76.8 (C, C-1), 75.9 (CH, C-5), 73.2 (C, C-4), 65.0 (CH, C-8), 63.1 (CH₂, C-13), 58.7 (CH₃, OCH₃-13), 36.0 (CH₂, C-3), 34.0 (CH₂, C-9), 30.9 (CH₂, C-2), 23.3 (CH₃, C-15), 23.0 (CH₃, OCOCH₃-10), 21.2 (CH₃, OCOCH₃-8), 20.5 (CH₃, OCOCH₃-5), and 19.8 (CH₃, C-14); HRESIMS: *m/z* 471.1859 [M+H]⁺ (calculated for C₂₂H₃₁O₁₁, 471.1866, error_{ppm} = −1.5).

Compound **3** was a pale yellow amorphous solid; LC-UV [acetonitrile in 0.1% aqueous formic acid] λ_{max} 225 nm; ¹H NMR (CDCl₃, 300 MHz, at 295 K): δ 5.92 (1H, s, H-5), 5.86 (1H, dd, *J* = 4.1, 2.4 Hz, H-8), 5.12 (1H, d, *J* = 12.9 Hz, H-13a), 4.79 (1H, d, *J* = 12.9 Hz, H-13b), 3.32 (1H, dd, *J* = 16.1, 2.4 Hz, H-9a), 2.42–2.30 (1H, m, H-2a), 2.39–2.25 (1H, m, H-3a), 2.22 (3H, s, OCOCH₃-10), 2.06 (1H, dd, *J* = 16.1, 4.1 Hz, H-9b), 2.05 (3H, s, OCOCH₃-13), 2.03 (3H, s, OCOCH₃-8), 1.98 (3H, s, OCOCH₃-5), 1.90–1.77 (1H, m, H-3b), 1.73–1.60 (1H, m, H-2b), 1.70 (3H, s, CH₃-14), and 1.41 (3H, s, CH₃-15); ¹³C NMR (CDCl₃, 75 MHz, at 295 K): δ 171.4 (CO, OCOCH₃-5), 170.7 (CO, OCOCH₃-8), 170.5 (CO, OCOCH₃-13), 170.4 (CO, C-12), 168.9 (CO, OCOCH₃-10), 157.4 (C, C-7), 128.0 (C, C-11), 89.4 (C, C-6), 84.2 (C, C-10), 76.8 (C, C-1), 75.9 (CH, C-5), 73.3 (C, C-4), 65.3 (CH, C-8), 55.0 (CH₂, C-13), 35.8 (CH₂, C-3), 33.8 (CH₂, C-9), 30.7 (CH₂, C-2), 23.3 (CH₃, C-15), 22.9 (CH₃, OCOCH₃-10), 21.2 (CH₃, OCOCH₃-8), 20.7 (CH₃, OCOCH₃-13), 20.4 (CH₃, OCOCH₃-5), and 19.7 (CH₃, C-14); HRESIMS: *m/z* 499.1794 [M+H]⁺ (calculated for C₂₃H₃₁O₁₂, 499.1816, error_{ppm} = −4.4).

For reaction condition *a(ii)*, DMAP (1.8 mg, 0.01 mmol, 0.2 molar eq.) was added to a solution of glaucolide B (**1**; 30.3 mg, 0.07 mmol, 1 molar eq.) in anhydrous CH₂Cl₂ (1 mL). The evolution of this reaction was monitored with TLC, and the mixture was stirred for 30 min at room temperature. The reaction mixture was concentrated under reduced

pressure and purified via silica gel CC using a gradient eluent system composed of acetone in *n*-hexane (20–100%, *v/v*), allowing the exclusive isolation of the semisynthetic derivative **3** (10.5 mg, 30.3%).

For the semisynthesis of 5,8-diacetoxy-2-epi-vernomargolide-1,4-cyclosemiacetal (**4**), 5,8,10-triacetoxy-2-epi-vernomargolide-1,4-cyclosemiacetal (**5**), and 5,8-diacetoxy-2-epi-vernomargolide-1,4-cycloacetal-1,10-acetonide (**6**), Ac₂O (108 μL, 1.14 mmol, 10.0 molar eq.) and BiCl₃ (161.8 mg, 0.51 mmol, 4.5 molar eq.) were added to a solution of glaucolide B (**1**; 50.0 mg, 0.11 mmol, 1 molar eq.) in anhydrous CH₂Cl₂ (1 mL) under an atmosphere of argon (Ar), and the mixture monitored with TLC was stirred for 2 h at room temperature (condition b). The reaction mixture was extracted with CH₂Cl₂ (3 × 15 mL) via liquid–liquid partition, and the organic layer was dried with anhydrous sodium sulfate (Na₂SO₄), filtered through filter paper, and concentrated under reduced pressure. The crude material was purified with silica gel CC using a gradient eluent system composed of acetone in CHCl₃ (10–30%, *v/v*) to produce the isolation of the semisynthetic derivatives **4** (11.1 mg, 24.6%), **5** (13.9 mg, 27.8%), and **6** (3.4 mg, 6.8%).

Compound **4** was a pale yellow amorphous solid; LC-UV [acetonitrile in 0.1% aqueous formic acid] λ_{max} 214 nm; ¹H NMR (CDCl₃, 300 MHz, at 295 K): δ 6.47 (1H, s, H-13a), 5.68 (1H, s, H-13b), 4.88 (1H, d, *J* = 5.4 Hz, H-5), 4.87 (1H, dd, *J* = 3.2, 2.8 Hz, H-8), 4.38 (1H, d, *J* = 5.4 Hz, H-6), 3.20 (1H, brs, OH-1), 2.80 (1H, d, *J* = 4.2 Hz, H-2), 2.59 (1H, dd, *J* = 12.6, 4.2 Hz, H-3a), 2.225 (1H, d, *J* = 3.2 Hz, H-9a), 2.200 (1H, d, *J* = 2.8 Hz, H-9b), 2.17 (3H, s, OCOCH₃-5), 2.07 (3H, s, OCOCH₃-8), 1.65 (1H, d, *J* = 12.6 Hz, H-3b), 1.60 (1H, brs, OH-10), 1.33 (3H, s, CH₃-14), and 1.31 (3H, s, CH₃-15); ¹³C NMR (CDCl₃, 75 MHz, at 295 K): δ 169.7 (CO, OCOCH₃-5), 168.6 (CO, OCOCH₃-8), 167.6 (CO, C-12), 136.8 (C, C-11), 125.5 (CH₂, C-13), 106.1 (C, C-1), 83.4 (CH, C-6), 83.2 (C, C-4), 80.0 (CH, C-5), 71.4 (C, C-10), 70.4 (CH, C-8), 50.5 (C, C-7), 43.8 (CH, C-2), 36.1 (CH₂, C-3), 35.0 (CH₂, C-9), 22.7 (CH₃, C-14), 22.0 (CH₃, C-15), 20.9 (CH₃, OCOCH₃-8), and 20.8 (CH₃, OCOCH₃-5); HRESIMS: *m/z* 419.1302 [M+Na]⁺ (calculated for C₁₉H₂₄O₉Na, 419.1318, error_{ppm} = −3.8).

Compound **5** was a pale yellow amorphous solid; LC-UV [acetonitrile in 0.1% aqueous formic acid] λ_{max} 218 nm; ¹H NMR (CDCl₃, 300 MHz, at 295 K): δ 6.46 (1H, s, H-13a), 5.66 (1H, s, H-13b), 4.90 (1H, d, *J* = 5.4 Hz, H-5), 4.84 (1H, dd, *J* = 3.2, 2.8 Hz, H-8), 4.36 (1H, d, *J* = 5.4 Hz, H-6), 3.26 (1H, dd, *J* = 16.8, 2.8 Hz, H-9a), 3.09 (1H, brs, OH-1), 2.80 (1H, d, *J* = 4.2 Hz, H-2), 2.62 (1H, dd, *J* = 12.7, 4.2 Hz, H-3a), 2.17 (3H, s, OCOCH₃-5), 2.09 (1H, dd, *J* = 16.6, 3.2 Hz, H-9b), 2.08 (3H, s, OCOCH₃-10), 1.99 (3H, s, OCOCH₃-8), 1.66 (3H, s, CH₃-14), 1.63 (1H, d, *J* = 12.7 Hz, H-3b), and 1.32 (3H, s, CH₃-15); ¹³C NMR (CDCl₃, 75 MHz, at 295 K): δ 169.9 (CO, OCOCH₃-5), 169.6 (CO, OCOCH₃-10), 168.8 (CO, OCOCH₃-8), 167.8 (CO, C-12), 136.8 (C, C-11), 125.5 (CH₂, C-13), 104.6 (C, C-1), 84.0 (CH, C-6), 83.3 (C, C-4), 81.3 (C, C-10), 80.0 (CH, C-5), 69.3 (CH, C-8), 50.4 (C, C-7), 44.5 (CH, C-2), 36.2 (CH₂, C-3), 30.4 (CH₂, C-9), 22.7 (CH₃, OCOCH₃-10), 22.0 (CH₃, C-15), 20.8 (CH₃, OCOCH₃-5), 20.6 (CH₃, OCOCH₃-8), and 19.1 (CH₃, C-14); HRESIMS: *m/z* 461.1409 [M+Na]⁺ (calculated for C₂₁H₂₆O₁₀Na, 461.1424, error_{ppm} = −3.3).

Compound **6** was a pale yellow amorphous solid; LC-UV [acetonitrile in 0.1% aqueous formic acid] λ_{max} 247 nm; ¹H NMR (CDCl₃, 300 MHz, at 295 K): δ 6.46 (1H, s, H-13a), 5.66 (1H, s, H-13b), 4.75 (1H, d, *J* = 6.0 Hz, H-5), 4.74 (1H, dd, *J* = 4.2, 2.3 Hz, H-8), 4.32 (1H, d, *J* = 6.0 Hz, H-6), 3.00 (1H, d, *J* = 4.6 Hz, H-2), 2.56 (1H, dd, *J* = 17.0, 2.3 Hz, H-9a), 2.32 (1H, dd, *J* = 12.8, 4.6 Hz, H-3a), 2.16 (3H, s, OCOCH₃-8), 2.03 (3H, s, OCOCH₃-5), 1.97 (1H, dd, *J* = 17.0, 4.2 Hz, H-9b), 1.79 (1H, d, *J* = 12.8 Hz, H-3b), 1.52 (3H, s, H-4'), 1.45 (3H, s, H-5'), 1.41 (3H, s, CH₃-14), and 1.29 (3H, s, CH₃-15); ¹³C NMR (CDCl₃, 75 MHz, at 295 K): δ 169.8 (CO, OCOCH₃-8), 169.4 (CO, OCOCH₃-5), 168.0 (CO, C-12), 136.8 (C, C-11), 125.1 (CH₂, C-13), 111.0 (C, C-1), 106.1 (C, C-2'), 82.3 (C, C-4), 81.7 (CH, C-6), 79.4 (CH, C-5), 76.4 (C, C-10), 69.4 (CH, C-8), 49.4 (C, C-7), 43.2 (CH, C-2), 35.5 (CH₂, C-9), 35.4 (CH₂, C-3), 29.4 (CH₃, C-4'), 28.8 (CH₃, C-5'), 25.5 (CH₃, C-14), 21.0 (CH₃, C-15), 20.8 (CH₃, OCOCH₃-8), and 20.7 (CH₃, OCOCH₃-5); HRESIMS: *m/z* 459.1624 [M+Na]⁺ (calculated for C₂₂H₂₈O₉Na, 459.1631, error_{ppm} = −1.5).

For the semisynthesis of 5-hydroxy-hirsutinolide (7), reaction condition *c(i)*, BiCl₃ (323.5 mg, 10.3 mmol, 4.5 molar eq.) was added to a solution of glaucolide B (1; 100.1 mg, 0.23 mmol, 1 molar eq.) in anhydrous CH₂Cl₂ (2 mL) under an atmosphere of argon (Ar), and the mixture monitored with TLC was stirred for 3 h at room temperature. The reaction mixture was extracted with CH₂Cl₂ (3 × 15 mL) via liquid–liquid partition and the organic layer was dried with anhydrous Na₂SO₄, filtered through filter paper, and concentrated under reduced pressure, producing compound 7 (80.5 mg, 77.4%). No further purification was necessary.

Compound 7 was a colorless amorphous solid; ¹H NMR (CDCl₃, 300 MHz, at 295 K): δ 5.90 (1H, dd, *J* = 3.5, 3.4 Hz, H-8), 5.11 (1H, d, *J* = 9.1 Hz, H-6), 4.91 (1H, d, *J* = 12.6 Hz, H-13a), 4.74 (1H, d, *J* = 12.6 Hz, H-13b), 4.30 (1H, brs, OH-1), 3.57 (1H, d, *J* = 9.1 Hz, H-5), 3.27 (1H, brs, OH-5), 2.58 (1H, dd, *J* = 15.6, 3.5 Hz, H-9a), 2.23–2.09 (2H, m, H-3a and H-3b), 2.18–2.08 (1H, m, H-2a), 2.15 (1H, d, *J* = 15.6 Hz, H-9b), 2.09 (3H, s, OCOCH₃-13), 2.06 (3H, s, OCOCH₃-8), 2.04 (3H, s, OCOCH₃-10), 1.88–1.78 (1H, m, H-2b), 1.62 (3H, s, CH₃-14), and 1.50 (3H, s, CH₃-15); ¹³C NMR (CDCl₃, 75 MHz, at 295 K): δ 171.7 (CO, OCOCH₃-10), 171.2 (CO, C-12), 170.3 (CO, OCOCH₃-13), 169.7 (CO, OCOCH₃-8), 168.6 (C, C-7), 123.1 (C, C-11), 108.8 (C, C-1), 87.0 (C, C-10), 86.5 (C, C-4), 82.0 (CH, C-6), 75.9 (CH, C-5), 68.4 (CH, C-8), 55.7 (CH₂, C-13), 41.8 (CH₂, C-9), 34.5 (CH₂, C-3), 33.9 (CH₂, C-2), 22.2 (CH₃, OCOCH₃-10), 21.9 (CH₃, C-15), 20.9 (CH₃, OCOCH₃-13), 20.6 (CH₃, OCOCH₃-8), and 17.5 (CH₃, C-14); HRESIMS: *m/z* 457.1686 [M+H]⁺ (calculated for C₂₁H₂₉O₁₁, 457.1710, error_{ppm} = −5.2).

For reaction condition *c(ii)*, TFA (10 μL, 0.13 mmol, 1.4 molar eq.) was added to a 1 mL solution of glaucolide B (1; 39.7 mg, 0.09 mmol, 1 molar eq.) in anhydrous CH₂Cl₂ at −2 °C. The reaction mixture monitored with TLC was stirred for 24 h at room temperature. A saturated NaHCO₃ aqueous solution (5 mL) was added to the reaction mixture, which was extracted with CHCl₃ (6 × 5 mL) via liquid–liquid partition, and the organic layer was dried with anhydrous Na₂SO₄, filtered through filter paper, and concentrated under reduced pressure. The crude material was purified via silica gel CC using an isocratic eluent composed of *n*-hexane/acetone (70:30, *v/v*), producing derivative 7 (15.5 mg, 37.5%), although with a lower reaction yield than *c(i)*.

For the semisynthesis of 1,8-diacetoxy-1(4),7(10)-diepoxy-5-hydroxygermacr-11(13)-en-6(12)-olide (8), 1N K₂CO₃ aqueous solution (725 μL, 0.36 mmol, 5.5 molar eq.) was added to a solution of 5-hydroxy-hirsutinolide (7; 30.0 mg, 0.07 mmol, 1 molar eq.) in THF (1.5 mL), and the mixture monitored with TLC was refluxed at 45 °C for 2 h (condition *d*). The reaction mixture was extracted with CH₂Cl₂ (3 × 15 mL) via liquid–liquid partition, and the organic layer was dried with anhydrous Na₂SO₄, filtered through filter paper, and concentrated under reduced pressure, yielding derivative 8 (8.8 mg, 33.7%). No further purification was necessary.

Compound 8 was a colorless amorphous solid; LC-UV [acetonitrile in 0.1% aqueous formic acid] λ_{max} 246 nm; ¹H NMR (CDCl₃, 300 MHz, at 295 K): δ 6.54 (1H, s, H-13a), 5.78 (1H, s, H-13b), 5.28 (1H, dd, *J* = 8.5, 7.5 Hz, H-8), 4.68 (1H, d, *J* = 10.3 Hz, H-6), 4.00 (1H, d, *J* = 10.3 Hz, H-5), 3.02 (1H, dd, *J* = 13.9, 8.5 Hz, H-9a), 2.63–2.51 (1H, m, H-2a), 2.63–2.51 (1H, m, H-3a), 2.27–2.17 (1H, m, H-2b), 2.15–1.97 (1H, m, H-3b), 2.04 (3H, s, OCOCH₃-1), 1.96 (3H, s, OCOCH₃-8), 1.89 (1H, dd, *J* = 13.9, 7.5 Hz, H-9b), 1.44 (3H, s, CH₃-15), and 1.38 (3H, s, CH₃-14); ¹³C NMR (CDCl₃, 75 MHz, at 295 K): δ 171.2 (CO, OCOCH₃-8), 168.2 (CO, OCOCH₃-1), 167.7 (CO, C-12), 136.9 (C, C-11), 129.4 (CH₂, C-13), 112.1 (C, C-1), 89.5 (C, C-7), 89.2 (C, C-4), 85.7 (C, C-10), 84.8 (CH, C-6), 82.8 (CH, C-8), 73.2 (CH, C-5), 40.1 (CH₂, C-9), 36.8 (CH₂, C-3), 31.6 (CH₂, C-2), 22.8 (CH₃, C-14), 22.3 (CH₃, OCOCH₃-1), 21.1 (CH₃, OCOCH₃-8), and 19.4 (CH₃, C-15); HRESIMS: *m/z* 397.1501 [M+H]⁺ (calculated for C₁₉H₂₅O₉, 397.1499, error_{ppm} = 0.5).

For the semisynthesis of 8-acetoxy-vernomargolide (9), BiCl₃ (106.1 mg, 0.34 mmol, 5.5 molar eq.) was added to a solution of 5-hydroxy-hirsutinolide (7; 28.0 mg, 0.06 mmol, 1 molar eq.) in anhydrous CH₂Cl₂ (2 mL), and the mixture was refluxed at 50 °C for 15 h (condition *e*). The reaction mixture monitored with TLC was extracted with CH₂Cl₂ (3 × 15 mL) via liquid–liquid partition, and the organic layer was dried with anhydrous

Na₂SO₄, filtered through filter paper, and concentrated under reduced pressure, providing derivative **9** (14.6 mg, 67.2%). No further purification was necessary. Compound **9** was a pale yellow amorphous solid; LC-UV [acetonitrile in 0.1% aqueous formic acid] λ_{max} 226 nm; ¹H NMR (CDCl₃, 300 MHz, at 295 K): δ 6.48 (1H, s, H-13a), 5.87 (1H, s, H-13b), 5.10 (1H, d, *J* = 5.5 Hz, H-8), 4.23 (1H, d, *J* = 4.6 Hz, H-6), 3.58 (1H, d, *J* = 4.6 Hz, H-5), 3.37 (1H, d, *J* = 4.4 Hz, H-2), 2.58 (1H, dd, *J* = 16.3, 5.5 Hz, H-9a), 2.30 (3H, s, CH₃-14), 2.23 (1H, d, *J* = 16.3 Hz, H-9b), 2.06 (3H, s, OCOCH₃-8), 1.78 (1H, dd, *J* = 13.4, 4.4 Hz, H-3a), 1.68 (1H, d, *J* = 13.4 Hz, H-3b), and 1.45 (3H, s, CH₃-15); ¹³C NMR (CDCl₃, 75 MHz, at 295 K): δ 209.4 (CO, C-1), 169.6 (CO, OCOCH₃-8), 168.6 (CO, C-12), 134.4 (C, C-11), 126.7 (CH₂, C-13), 96.5 (C, C-10), 87.4 (CH, C-6), 84.4 (C, C-4), 79.6 (CH, C-8), 79.1 (CH, C-5), 56.7 (C, C-7), 53.4 (CH, C-2), 43.2 (CH₂, C-9), 35.9 (CH₂, C-3), 26.5 (CH₃, C-14), 21.2 (CH₃, C-15), and 20.9 (CH₃, OCOCH₃-8); HRESIMS: *m/z* 355.1396 [M+H]⁺ (calculated for C₁₇H₂₃O₈, 355.1393, error_{ppm} = 0.8).

For the semisynthesis of 5-acetoxy-hirsutinolide (**7a**), 1,5,8-triacetoxy-1(4),7(10)-diepoxy-germacr-11(13)-en-6(12)-olide (**8a**), and 5,8-diacetoxy-vernomargolide (**9a**), one-pot, two-step acetylation reactions were performed via the semisynthetic derivatives **7**, **8**, and **9**. Therefore, as an acetylation general condition, DMAP (0.05 molar eq.) was added to a suspension of Ac₂O (1–3 molar eq.) and Et₃N (1.5–3.5 molar eq.) in anhydrous CH₂Cl₂ (1 mL), and the mixture was stirred at –10 °C for 30 min. After that, each respective SL semisynthetic derivative (**7**, **8**, or **9**) was added to the mixture, which was stirred for 30 min at room temperature (condition f). Water (3 mL) was added to each reaction mixture, which were monitored with TLC while stirring for 30 min at room temperature. Thereafter, the mixture was extracted with CH₂Cl₂ (3 × 15 mL) via liquid–liquid partition. The organic layer was dried with anhydrous Na₂SO₄, filtered through filter paper, and concentrated under reduced pressure.

For the acetylation reaction of compound **7** (30.0 mg, 0.07 mmol, 1 molar eq.), DMAP (0.4 mg, 0.003 mmol), Ac₂O (6 μL, 0.07 mmol, 1 molar eq.), and Et₃N (14 μL, 0.10 mmol, 1.5 molar eq.) were used. The mixture was monitored with TLC while stirring for 0.5 h at room temperature. After the complete consumption of compound **7**, the obtained crude material was purified via silica gel CC using gradient eluent systems composed of acetone in *n*-hexane (30–50%, *v/v*) to obtain the isolation of the C-5 acetylated derivative **7a** (12.4 mg, 37.8%). Compound **7a** was a colorless amorphous solid; LC-UV [acetonitrile in 0.1% aqueous formic acid] λ_{max} 225 nm; ¹H NMR (CDCl₃, 300 MHz, at 308 K): δ 5.92 (1H, dd, *J* = 3.7, 3.5 Hz, H-8), 5.10 (1H, d, *J* = 9.5 Hz, H-6), 4.96–4.88 (1H, m, H-5), 4.92 (1H, d, *J* = 12.7 Hz, H-13a), 4.74 (1H, d, *J* = 12.7 Hz, H-13b), 2.58 (1H, dd, *J* = 15.5, 3.7 Hz, H-9a), 2.33–2.17 (1H, m, H-2a), 2.14 (3H, s, OCOCH₃-5), 2.13–1.98 (1H, m, H-3a), 2.09 (3H, s, OCOCH₃-13), 2.09–2.04 (1H, m, H-9b), 2.05 (3H, s, OCOCH₃-8), 2.04 (3H, s, OCOCH₃-10), 1.93–1.82 (1H, m, H-3b), 1.88–1.77 (1H, m, H-2b), 1.62 (3H, s, CH₃-14), and 1.56 (3H, s, CH₃-15); ¹³C NMR (CDCl₃, 75 MHz, at 308 K): δ 171.4 (CO, OCOCH₃-10), 170.2 (CO, OCOCH₃-5), 170.2 (CO, C-12), 170.1 (CO, OCOCH₃-13), 169.5 (CO, OCOCH₃-8), 166.5 (C, C-7), 124.0 (C, C-11), 109.5 (C, C-1), 86.7 (C, C-10), 85.0 (C, C-4), 79.4 (CH, C-6), 73.4 (CH, C-5), 68.3 (CH, C-8), 55.7 (CH₂, C-13), 41.2 (CH₂, C-9), 34.3 (CH₂, C-3), 33.6 (CH₂, C-2), 22.4 (CH₃, C-15), 22.1 (CH₃, OCOCH₃-10), 20.8 (CH₃, OCOCH₃-13), 20.6 (CH₃, OCOCH₃-5), 20.5 (CH₃, OCOCH₃-8), and 17.6 (CH₃, C-14); HRESIMS: *m/z* 499.1794 [M+H]⁺ (calculated for C₂₃H₃₁O₁₂, 499.1816, error_{ppm} = –4.4).

Compound **8** (7.7 mg, 0.02 mmol, 1 molar eq.), in turn, was treated with DMAP (0.1 mg, 0.001 mmol), Ac₂O (2 μL, 0.02 mmol, 1 molar eq.), and Et₃N (4 μL, 0.03 mmol, 1.5 molar eq.). After completion of the reaction as determined via TLC (0.5 h), the corresponding crude material was purified with preparative TLC using an isocratic eluent system composed of *n*-hexane/acetone (70:30, *v/v*; R_f ≈ 0.40), producing the isolated C-5 acetylated derivative **8a** (1.6 mg, 18.8%). Compound **8a** was a colorless amorphous solid; LC-UV [acetonitrile in 0.1% aqueous formic acid] λ_{max} 246 nm; ¹H NMR (CDCl₃, 300 MHz, at 295 K): δ 6.51 (1H, s, H-13a), 5.79 (1H, s, H-13b), 5.33 (1H, d, *J* = 10.4 Hz, H-5), 5.28 (1H, dd, *J* = 8.3, 6.2 Hz, H-8), 4.67 (1H, d, *J* = 10.4 Hz, H-6), 3.02 (1H, dd, *J* = 14.2, 8.3 Hz, H-9a), 2.76–2.62 (1H,

m, H-2a), 2.58–2.46 (1H, m, H-3a), 2.27–2.17 (1H, m, H-2b), 2.11 (3H, s, OCOCH₃-5), 2.04 (3H, s, OCOCH₃-1), 1.96 (3H, s, OCOCH₃-8), 1.94–1.87 (1H, m, H-3b), 1.91 (1H, dd, *J* = 14.2, 6.2 Hz, H-9b), 1.45 (3H, s, CH₃-15), and 1.41 (3H, s, CH₃-14); ¹³C NMR (CDCl₃, 75 MHz, at 295 K): δ 170.6 (CO, OCOCH₃-8), 170.0 (CO, OCOCH₃-5), 168.0 (CO, OCOCH₃-1), 167.2 (CO, C-12), 135.8 (C, C-11), 128.7 (CH₂, C-13), 112.0 (C, C-1), 89.7 (C, C-7), 87.2 (C, C-4), 85.5 (C, C-10), 81.8 (CH, C-8), 81.4 (CH, C-6), 71.9 (CH, C-5), 39.6 (CH₂, C-9), 36.5 (CH₂, C-3), 31.2 (CH₂, C-2), 22.6 (CH₃, C-14), 22.0 (CH₃, OCOCH₃-1), 20.8 (CH₃, OCOCH₃-8), 20.6 (CH₃, OCOCH₃-5), and 20.0 (CH₃, C-15); HRESIMS: *m/z* 439.1612 [M+H]⁺ (calculated for C₂₁H₂₇O₁₀, 439.1604, error_{ppm} = 1.8).

Compound **9** (12.0 mg, 0.03 mmol, 1 molar eq.) was subjected to acetylation reaction using DMAP (0.2 mg, 0.002 mmol), Ac₂O (10 μL, 0.10 mmol, 3 molar eq.), and Et₃N (16 μL, 0.12 mmol, 3.5 molar eq.). The medium was stirred at room temperature and the reaction was stopped within 0.5 h after the complete consumption of the substrate as revealed via TLC. The medium was extracted using an immiscible liquid–liquid separation process with CH₂Cl₂ (3 × 15 mL). After the filtration and evaporation of CH₂Cl₂, compound **9a** was obtained (8.8 mg, 65.7%). Compound **9a** was a colorless amorphous solid; LC-UV [acetonitrile in 0.1% aqueous formic acid] λ_{max} 246 nm; ¹H NMR (CDCl₃, 300 MHz, at 295 K): δ 6.50 (1H, s, H-13a), 5.84 (1H, s, H-13b), 5.10 (1H, d, *J* = 5.6 Hz, H-8), 4.90 (1H, d, *J* = 6.2 Hz, H-5), 4.30 (1H, d, *J* = 6.2 Hz, H-6), 3.46 (1H, dd, *J* = 3.5, 1.4 Hz, H-2), 2.65 (1H, dd, *J* = 16.4, 5.6 Hz, H-9a), 2.29 (3H, s, CH₃-14), 2.19 (3H, s, OCOCH₃-5), 2.18 (1H, d, *J* = 16.4 Hz, H-9b), 2.04 (3H, s, OCOCH₃-8), 1.82 (1H, d, *J* = 1.4 Hz, H-3a), 1.81 (1H, d, *J* = 3.5 Hz, H-3b), and 1.30 (3H, s, CH₃-15); ¹³C NMR (CDCl₃, 75 MHz, at 295 K): δ 208.8 (CO, C-1), 169.5 (CO, OCOCH₃-5), 169.3 (CO, OCOCH₃-8), 167.8 (CO, C-12), 133.3 (C, C-11), 126.3 (CH₂, C-13), 96.6 (C, C-10), 83.8 (C, C-4), 83.7 (CH, C-6), 79.3 (CH, C-5), 78.8 (CH, C-8), 56.4 (C, C-7), 52.0 (CH, C-2), 42.5 (CH₂, C-9), 36.2 (CH₂, C-3), 26.2 (CH₃, C-14), 20.6 (CH₃, OCOCH₃-8), 20.6 (CH₃, C-15), and 20.5 (CH₃, OCOCH₃-5); HRESIMS: *m/z* 397.1501 [M+H]⁺ (calculated for C₁₉H₂₅O₉, 397.1499, error_{ppm} = 0.5).

For the semisynthesis of 8,10,13-triacetoxy-1(4)-epoxy-germacra-1(2),5(6),7(11)-trien-6(12)-olide (**7b**), pyridine (8 μL, 0.10 mmol, 1.5 molar eq.) was added to a solution of 5-hydroxy-hirsutinolide (**7**; 30.2 mg, 0.07 mmol, 1 molar eq.) in anhydrous CH₂Cl₂ (1.5 mL) under an atmosphere of argon at −10 °C. After that, SOCl₂ (35 μL, 0.48 mmol, 7.3 molar eq.) diluted in 300 μL of anhydrous CH₂Cl₂ was added dropwise to the mixture, which was stirred under the same condition for 30 min. Then, the mixture monitored with TLC was refluxed at 60 °C for 3.5 h (condition g). The reaction mixture was concentrated under reduced pressure, and the resulting crude material was purified via SPE using silica gel as a stationary phase and CH₂Cl₂ as an eluent, obtaining derivative **7b** (11.1 mg, 40.1%). Compound **7b** was a pale yellow amorphous solid; LC-UV [acetonitrile in 0.1% aqueous formic acid] λ_{max} 279 nm; ¹H NMR (CDCl₃, 300 MHz, at 295 K): δ 6.83 (1H, d, *J* = 8.3 Hz, H-8), 5.70 (1H, s, H-5), 5.12 (1H, d, *J* = 12.9 Hz, H-13a), 4.87 (1H, d, *J* = 12.9 Hz, H-13b), 4.82 (1H, dd, *J* = 3.2, 1.3 Hz, H-2), 3.08 (1H, d, *J* = 14.2 Hz, H-9a), 2.78 (1H, dd, *J* = 15.4, 1.3 Hz, H-3a), 2.49 (1H, dd, *J* = 15.4, 3.2 Hz, H-3b), 2.33 (1H, dd, *J* = 14.2, 8.3 Hz, H-9b), 2.09 (3H, s, OCOCH₃-8), 2.08 (3H, s, OCOCH₃-13), 2.04 (3H, s, OCOCH₃-10), 1.81 (3H, s, CH₃-14), and 1.72 (3H, s, CH₃-15); ¹³C NMR (CDCl₃, 75 MHz, at 295 K): δ 170.2 (CO, OCOCH₃-13), 169.25 (CO, OCOCH₃-10), 169.20 (CO, OCOCH₃-8), 167.2 (CO, C-12), 157.8 (C, C-1), 153.6 (C, C-7), 144.8 (C, C-6), 127.2 (C, C-11), 123.2 (CH, C-5), 94.1 (CH, C-2), 85.8 (C, C-4), 77.9 (C, C-10), 66.2 (CH, C-8), 56.4 (CH₂, C-13), 49.3 (CH₂, C-9), 42.4 (CH₂, C-3), 25.2 (CH₃, C-15), 22.1 (CH₃, OCOCH₃-10), 21.1 (CH₃, C-14), 20.9 (CH₃, OCOCH₃-13), and 20.8 (CH₃, OCOCH₃-8); HRESIMS: *m/z* 443.1301 [M+Na]⁺ (calculated for C₂₁H₂₄O₉Na, 443.1318, error_{ppm} = −3.8).

For the semisynthesis of 8,10,13-triacetoxy-1(4)-epoxy-6-hydroxy-5-keto-germacr-7(11)-en-6(12)-olide (**7c**), 226.6 mg of a mixture (1:1, m/m) of PCC (113.3 mg, 0.52 mmol, 8 molar eq.) and silica gel was added to a solution of 5-hydroxy-hirsutinolide (**7**; 30.0 mg, 0.07 mmol, 1 molar eq.) in anhydrous CH₂Cl₂ (2 mL) under an atmosphere of argon, and the mixture was monitored with TLC. The reaction under a stirring condition was completed within 48 h at room temperature (condition h). The reaction mixture was dried under reduced

pressure, and the obtained crude material was purified via silica gel CC using an isocratic eluent condition of $\text{CH}_2\text{Cl}_2/\text{acetone}$ (80:20, *v/v*) to obtain derivative **7c** (20.1 mg, 63.3%). Compound **7c** was a pale yellow amorphous solid; LC-UV [acetonitrile in 0.1% aqueous formic acid] λ_{max} 243 and 299 nm; ^1H NMR (CDCl_3 , 300 MHz, at 278 K): δ 6.81 (1H, s, OH-6), 6.36 (1H, dd, $J = 11.7, 6.4$ Hz, H-8), 4.84 (1H, d, $J = 12.7$ Hz, H-13a), 4.71 (1H, d, $J = 12.7$ Hz, H-13b), 3.32 (1H, dd, $J = 14.3, 11.7$ Hz, H-9a), 2.69–2.56 (1H, m, H-3a), 2.60 (1H, dd, $J = 14.3, 6.4$ Hz, H-9b), 2.54–2.42 (1H, m, H-2a), 2.12–1.99 (1H, m, H-3b), 2.094 (3H, s, OCOCH_3 -13), 2.090 (3H, s, OCOCH_3 -8), 2.04 (3H, s, OCOCH_3 -10), 2.01–1.86 (1H, m, H-2b), 1.75 (3H, s, CH_3 -15), and 1.61 (3H, s, CH_3 -14); ^{13}C NMR (CDCl_3 , 75 MHz, at 278 K): δ 200.9 (CO, C-5), 173.0 (CO, OCOCH_3 -8), 170.0 (CO, OCOCH_3 -13), 169.4 (CO, OCOCH_3 -10), 167.6 (CO, C-12), 162.7 (C, C-7), 127.9 (C, C-11), 111.1 (C, C-1), 107.6 (C, C-6), 87.2 (C, C-4), 86.5 (C, C-10), 68.2 (CH, C-8), 55.0 (CH_2 , C-13), 36.9 (CH_2 , C-3), 35.1 (CH_2 , C-9), 34.9 (CH_2 , C-2), 28.3 (CH_3 , C-15), 21.7 (CH_3 , C-14), 21.0 (CH_3 , OCOCH_3 -10), 20.8 (CH_3 , OCOCH_3 -8), and 20.8 (CH_3 , OCOCH_3 -13); HRESIMS: m/z 471.1504 $[\text{M}+\text{H}]^+$ (calculated for $\text{C}_{21}\text{H}_{27}\text{O}_{12}$, 471.1503, $\text{error}_{\text{ppm}} = 0.2$).

For the semisynthesis of 8,10-diacetoxy-4(7)-epoxy-6-hydroxy-1,5-diketo-germacr-11(13)-en-6(12)-olide (**7c.1**), BiCl_3 (76.3 mg, 0.24 mmol, 5.5 molar eq.) was added to a solution of compound **7c** (20.0 mg, 0.04 mmol, 1 molar eq.) in anhydrous CH_2Cl_2 (2 mL), and the mixture was refluxed at 50 °C and monitored with TLC. The starting material was consumed completely within 15 h (condition *e*). The reaction mixture was extracted with CH_2Cl_2 (3×15 mL) via liquid–liquid partition. The organic layer was dried with anhydrous Na_2SO_4 , filtered through filter paper, and the solvent was evaporated under reduced pressure. The crude material was purified with preparative TLC using an isocratic eluent mixture composed of *n*-hexane/acetone (60:40, *v/v*; $R_f \cong 0.46$), obtaining derivative **7c.1** (2.3 mg, 13.2%). Compound **7c.1** was a colorless amorphous solid; LC-UV [acetonitrile in 0.1% aqueous formic acid] λ_{max} 245 nm; ^1H NMR (CDCl_3 , 300 MHz, at 295 K): δ 6.58 (1H, d, $J = 0.7$ Hz, H-13a), 6.06 (1H, d, $J = 0.7$ Hz, H-13b), 5.28 (1H, d, $J = 9.5$ Hz, H-8), 4.90 (1H, brs, OH-6), 2.63 (1H, dd, $J = 16.0, 9.5$ Hz, H-9a), 2.62–2.49 (1H, m, H-3a), 2.54–2.41 (1H, m, H-2a), 2.26–2.14 (1H, m, H-3b), 2.05 (1H, d, $J = 16.0$ Hz, H-9b), 2.03–1.93 (1H, m, H-2b), 2.02 (3H, s, OCOCH_3 -8), 2.01 (3H, s, OCOCH_3 -10), 1.71 (3H, s, CH_3 -14), and 1.28 (3H, s, CH_3 -15); ^{13}C NMR (CDCl_3 , 75 MHz, at 295 K): δ 205.6 (CO, C-5), 203.9 (CO, C-1), 169.5 (CO, OCOCH_3 -10), 169.1 (CO, OCOCH_3 -8), 166.0 (CO, C-12), 136.4 (C, C-11), 129.7 (CH_2 , C-13), 99.3 (C, C-6), 84.5 (C, C-10), 83.9 (C, C-4), 82.2 (C, C-7), 66.9 (CH, C-8), 40.7 (CH_2 , C-9), 34.3 (CH_2 , C-3), 29.5 (CH_2 , C-2), 26.2 (CH_3 , C-15), 21.1 (CH_3 , OCOCH_3 -10), 20.9 (CH_3 , OCOCH_3 -8), and 18.3 (CH_3 , C-14); HRESIMS: m/z 411.1279 $[\text{M}+\text{H}]^+$ (calculated for $\text{C}_{19}\text{H}_{23}\text{O}_{10}$, 411.1291, $\text{error}_{\text{ppm}} = -2.9$). (For details on UV, NMR, and HRESIMS of all semisynthetic derivatives, see the Supplementary Materials).

3.3. Computational Calculation

The structures of the semisynthetic derivatives were drawn using the software *Marvin 19.1.11.0* [66]. The software *Standardizer JChem 16.1.11.0* [67] was used to canonize the structures. This process used a divide-and-conquer approach and converted an arbitrarily chosen chemical structure into a unique notation, added hydrogens, and cleaned the molecular graph in three dimensions. The structure was split into small fragments that were organized into a tree using connectivity information. Conformers generated for the initial structure (represented by the root node in the tree) were optimized. The tree-building process used a proprietary extended version of the Dreiding force field [68]. Geometric optimizations and conformational searches were performed using *Spartan 16* for Windows software [69]. The geometry of the chemical structure of each compound was initially optimized with a Merck molecular force field [70], and a new geometric optimization was then performed based on the PM6 semi-empirical method [71]. A systematic search method was used to analyze conformers and select that with the lowest minimum energy using AM1 and a Monte-Carlo algorithm [72]. After that, minimum energies were selected and optimized based on a vibrational mode calculation using density functional theory (DFT) [73].

DFT calculations were performed using the software *Spartan 16* for *Windows* (Wavefunction, Irvine, CA, USA) [73,74]. Each structure studied was examined at the B3LYP/6-31G* level, and the lowest energy structures were selected for the calculations [73,74]. The global minimum on the potential energy surface was used for the determination of each geometry.

3.4. Biological Assay

To evaluate the potential antitumoral activity of the compounds, the MTT [3-(4,5-dimethyl-2-thiazolyl)-2,5-diphenyl-2H-tetrazolium bromide] method [75] was used to determine the cell viability of SK-MEL-28 (human melanoma cell line), NCI-H460 (human lung carcinoma cell line), SF295 (human glioblastoma cell line), and HUVEC (human umbilical vein endothelial cells) line. Cell viability analysis of murine macrophage J774A.1 was conducted using a resazurin-based cytotoxicity assay (Alamar blue[®]) [76]. All cell lines were acquired from the BCRJ (Rio de Janeiro Cell Bank, Federal University of Rio de Janeiro, Brazil). The cell lines were cultivated in RPMI-1640 or DMEM medium, supplemented with 1.5 g/L of sodium bicarbonate, 10 mM of HEPES, pH 7.4, 100 U/mL of penicillin G, 100 µg/mL of streptomycin, and 10% fetal calf serum at 37 °C in a humidified atmosphere consisting of 95% air and 5% CO₂ cultures, and greater than 95% of viable cells in trypan blue exclusion tests were used for the experiments. Therefore, cells were seeded (1×10^4 /well) in 96-well plates and incubated with increasing concentrations of the compounds for 24 h. After incubation, the former culture medium was replaced with a fresh culture medium with 5 mg/mL of MTT and with 0.1 mg/mL of resazurin for 2 h at 37 °C. MTT formazan crystals were dissolved in DMSO, and the absorbance of each well was measured at 540 nm, using a micro-well system reader. For the control group of each cell line, cells were incubated without the compounds and considered to have 100% cell viability. MTT formazan crystals were dissolved in DMSO, and absorbance was measured at 540 nm using a microplate reader (ELX800, Biotek, Winooski, VT, USA). The half-maximal cytotoxic concentration (CC₅₀) values were calculated from a Hill concentration–response curve. Results were expressed as the mean \pm SD of three experiments. The selectivity index (SI) was calculated via the ratio between the CC₅₀ of non-tumoral cells and the tumoral cell lines. The higher the SI value is, the more selective the compound is to the tumoral cell line. For the resazurin assay, fluorescence was measured at 1 h intervals using a plate multi-reader (Infinite Multireader m200 Tecan) at 530–590 nm. Nonlinear regression of each fraction versus percentage cell viability was performed to obtain a 10% toxicity concentration (a concentration causing 90% cell viability) using GraphPad Prism 8.0 software (GraphPad Software, San Diego, CA, USA).

The *in vitro* anti-inflammatory activity was performed in murine macrophage J774A.1 and analyzed after modifications to the protocol previously described by Herath and coworkers [77]. The evaluation consisted of measuring the production of nitrite through an indicator of NO synthesis in supernatants from LPS-activated macrophages. A number of 1×10^5 cells/well were seeded in 96-well plates for 24 h, after which time the culture medium was changed, and the CC₁₀ concentration (Figure S70, found in the Supplementary Materials) of each compound was added to the medium containing DMEM supplemented with 10% FBS. After 15 min, macrophages were stimulated with 10 µg/mL of LPS and incubated for 24 h to obtain a proinflammatory M1-phenotype. Subsequently, supernatants were collected and total nitrite nitrate (NO_x) was measured by adding 100 µL of Griess' reagent (1% sulfanilamide and 0.1% *N*-(1-naphthyl) ethylenediamine in 0.5% phosphoric acid) [78]. Absorbance was determined with a microplate reader (ELX800, BioTek, Winooski, VT, USA) at 540 nm. In addition, the proinflammatory cytokine IL-6 was determined using an enzyme-linked immunosorbent assay (ELISA) (BD Bioscience, San Jose, CA, USA) according to the manufacturer's instructions.

4. Conclusions

The use of five different acid and basic catalysts, associated with complementary reaction conditions, allowed the production of fourteen semisynthetic SL-derivatives,

including ten new compounds (**4**, **5**, **6**, **7a**, **7c**, **7c.1**, **8**, **8a**, **9**, and **9a**), whose different carbocyclic cores were formed via rearrangement reactions and transannular cyclization. As shown in Figure 2, basic conditions favored the formation of the vernojalcanolide-type (cadinanolides **2** and **3**), and acidic conditions allowed the formation of the hirsutinolide (**7**) and the vernomargolide-type (cadinanolides **4**, **5**, and **6**) from the natural SL glaucolide B (**1**). Furthermore, when subjected to acidic conditions, the hirsutinolide derivative (**7**) allowed the formation of a vernomargolide-type (cadinanolide **9**), and under basic conditions, germacranolide core (**8**) formation was favored.

Regarding antiproliferative activity, hirsutinolides **7a** ($CC_{50} = 5.0 \mu\text{M}$, $SI = 2.5$) and **7b** ($CC_{50} = 11.2 \mu\text{M}$, $SI = 2.5$) and germacranolide **8a** ($CC_{50} = 3.1 \mu\text{M}$, $SI = 3.0$) turned out to be the most active against SK-MEL-28 human melanoma cells. The cytotoxic activity seems to improve as the lipophilicity of these compounds increases compared with the starting material after acetylation reactions. With all compounds showing an anti-inflammatory effect to some degree, compounds **7a** and **7c.1** were the most active with the greatest reduction (of about 77%) in NOx and IL-6 levels in pre-treated M1 macrophages.

Supplementary Materials: The following supporting information can be downloaded at <https://www.mdpi.com/article/10.3390/molecules28031243/s1>: NMR, HRESIMS, and UV spectra of the semisynthetic SL derivatives (Figures S1–S69), and the evaluation of the cell viability of macrophage J774A.1 treated with SLs (Figure S70).

Author Contributions: Conceptualization, L.A.L.d.S., L.P.S., and M.W.B.; methodology, L.A.L.d.S. and L.P.S.; formal analysis, L.A.L.d.S., L.S.A., A.N.P., C.D.d.S., M.T.S., L.S., and F.B.F.-M.; investigation, L.A.L.d.S., L.S.A., A.N.P., and C.D.d.S.; writing—original draft preparation, L.A.L.d.S. and L.P.S.; writing—review and editing, L.A.L.d.S., T.B.C.-P., M.T.S., L.S., F.B.F.-M., L.P.S., and M.W.B.; visualization, L.A.L.d.S., L.S.A., A.N.P., C.D.d.S., T.B.C.-P., M.T.S., and F.B.F.-M.; supervision, L.P.S. and M.W.B.; project administration, M.W.B.; funding acquisition, L.P.S. and M.W.B. All authors have read and agreed to the published version of the manuscript.

Funding: This study was financed in part by the Coordenação de Aperfeiçoamento de Pessoal de Nível Superior–Brasil (CAPES), finance code 001.

Institutional Review Board Statement: Not applicable.

Informed Consent Statement: Not applicable.

Data Availability Statement: Not applicable.

Acknowledgments: The authors acknowledge the Coordenação de Aperfeiçoamento de Pessoal de Nível Superior–Brasil (CAPES) for their financial support.

Conflicts of Interest: The authors declare no conflict of interest.

Sample Availability: Samples of the compounds are not available from the authors.

References

1. Padilla-Gonzalez, G.F.; dos Santos, F.A.; Da Costa, F.B. Sesquiterpene lactones: More than protective plant compounds with high toxicity. *CRC Crit. Rev. Plant Sci.* **2016**, *35*, 18–37. [[CrossRef](#)]
2. Da Costa, F.B.; Terfloth, L.; Gasteiger, J. Sesquiterpene lactone-based classification of three Asteraceae tribes: A study based on self-organizing neural networks applied to chemosystematics. *Phytochemistry* **2005**, *66*, 345–353. [[CrossRef](#)]
3. Loeuille, B.; Keeley, S.C.; Pirani, J.R. Systematics and evolution of syncephaly in American Vernoniae (Asteraceae) with emphasis on the Brazilian subtribe Lychnophorinae. *Syst. Bot.* **2015**, *40*, 286–298. [[CrossRef](#)]
4. Gallon, M.E.; Jaiyesimi, O.A.; Gobbo-Neto, L. LC-UV-HRMS dereplication of secondary metabolites from Brazilian Vernoniae (Asteraceae) species supported through *in-house* database. *Biochem. Syst. Ecol.* **2018**, *78*, 5–16. [[CrossRef](#)]
5. Jakupovic, J.; Gage, D.A.; Bohlmann, F.; Mabry, T.J. Sesquiterpene lactones from *Vernonia marginata*. *Phytochemistry* **1986**, *25*, 1179–1183. [[CrossRef](#)]
6. Pillay, P.; Vleggaar, R.; Maharaj, V.J.; Smith, P.J.; Lategan, C.A.; Chouteau, F.; Chibale, K. Antiplasmodial hirsutinolides from *Vernonia staehelinoides* and their utilization towards a simplified pharmacophore. *Phytochemistry* **2007**, *68*, 1200–1205. [[CrossRef](#)]
7. Appezato-da-Gloria, B.; Da Costa, F.B.; da Silva, V.C.; Gobbo-Neto, L.; Rehder, V.L.G.; Hayashi, A.H. Glandular trichomes on aerial and underground organs in *Chrysolaena* species (Vernoniae—Asteraceae): Structure, ultrastructure and chemical composition. *Flora* **2012**, *207*, 878–887. [[CrossRef](#)]

8. Bardón, A.; Montanaro, S.; Catalán, C.A.N.; Diaz, J.G.; Herz, W. Piptocarphols and other constituents of *Chrysolaena verbascifolia* and *Lessingianthus rubricaulis*. *Phytochemistry* **1993**, *34*, 253–259. [[CrossRef](#)]
9. Borkosky, S.; Bardón, A.; Catalán, C.A.N.; Diaz, J.G.; Herz, W. Glaucolides, hirsutinolides and other sesquiterpene lactones from *Vernonanthura pinguis*. *Phytochemistry* **1997**, *44*, 465–470. [[CrossRef](#)]
10. Buskuhl, H.; de Oliveira, F.L.; Blind, L.Z.; de Freitas, R.A.; Barison, A.; Campos, F.R.; Corilo, Y.E.; Eberlin, M.N.; Caramori, G.F.; Biavatti, M.W. Sesquiterpene lactones from *Vernonia scorpioides* and their *in vitro* cytotoxicity. *Phytochemistry* **2010**, *71*, 1539–1544. [[CrossRef](#)]
11. Tully, L.E.; Carson, M.S.; McMurry, T.B.H. A novel sesquiterpene lactone from *Vernonia erinacea*. *Tetrahedron Lett.* **1987**, *28*, 5925–5928. [[CrossRef](#)]
12. Martínez, V.M.; Sánchez, F.A.; López, B.G.; Joseph-Nathan, P. Rearrangement of glaucolide A into vernojalcanolide 8-O-methacrylate. *Z. Naturforsch. C* **1986**, *41*, 1119–1120.
13. Bazon, J.N.; Lopes, J.L.C.; Vichnewski, W.; Dias, D.A.; Nagamiti, K.; Cunha, W.R.; Herz, W. Cadinanolides and other constituents from *Vernonia fruticulosa* and *Vernonanthura discolor*. *Phytochemistry* **1997**, *44*, 1535–1536. [[CrossRef](#)]
14. Martínez-Vázquez, M.; Sepúlveda, S.; Belmont, M.A.; Rubio, M.; Joseph-Nathan, P. The transformation of glaucolide A into cadinanolides and hirsutinolides. *J. Nat. Prod.* **1992**, *55*, 884–898. [[CrossRef](#)]
15. Flores-Guzmán, F.; Alvarado-Sansininea, J.J.; López-Muñoz, H.; Escobar, M.L.; Espinosa-Trejo, M.; Tavera-Hernandez, R.; Jiménez-Estrada, M.; Sánchez-Sánchez, L. Antiproliferative, cytotoxic and apoptotic activity of the bentonite transformation of sesquiterpene lactone glaucolide B to 5 β -hydroxy-hirsutinolide on tumor cell lines. *Eur. J. Pharmacol.* **2019**, *856*, 172406. [[CrossRef](#)]
16. Ramos, A.V.G.; Peixoto, J.L.B.; Cabral, M.R.P.; Amrein, A.M.; Tiunan, T.S.; Cottica, S.M.; Souza, I.M.O.; Ruiz, A.L.T.G.; Foglio, M.A.; Carmo, M.R.B. Chemical constituents, antiproliferative and antioxidant activities of *Vernonanthura nudiflora* (Less.) H. Rob. aerial parts. *J. Braz. Chem. Soc.* **2019**, *30*, 1728–1740. [[CrossRef](#)]
17. Zhang, M.; Yang, X.; Wei, Y.; Wall, M.; Songsak, T.; Wongwiwatthananukit, S.; Chang, L.C. Bioactive sesquiterpene lactones isolated from the whole plants of *Vernonia cinerea*. *J. Nat. Prod.* **2019**, *82*, 2124–2131. [[CrossRef](#)] [[PubMed](#)]
18. Chea, A.; Hout, S.; Long, C.; Marcourt, L.; Faure, R.; Azas, N.; Elias, R. Antimalarial activity of sesquiterpene lactones from *Vernonia cinerea*. *Chem. Pharm. Bull.* **2006**, *54*, 1437–1439. [[CrossRef](#)]
19. Youn, U.J.; Park, E.-J.; Kondratyuk, T.P.; Simmons, C.J.; Borris, R.P.; Tanamatayarat, P.; Wongwiwatthananukit, S.; Toyama, O.; Songsak, T.; Pezzuto, J.M. Anti-inflammatory sesquiterpene lactones from the flower of *Vernonia cinerea*. *Bioorg. Med. Chem. Lett.* **2012**, *22*, 5559–5562. [[CrossRef](#)]
20. Kuo, L.-M.Y.; Tseng, P.-Y.; Lin, Y.-C.; Liaw, C.-C.; Zhang, L.-J.; Tsai, K.-C.; Lin, Z.-H.; Ho, H.-O.; Kuo, Y.-H. New hirsutinolide-type sesquiterpenoids from *Vernonia cinerea* inhibit nitric oxide production in LPS-stimulated RAW 264. 7 cells. *Planta Med.* **2018**, *84*, 1348–1354.
21. Yang, Y.-L.; Chang, S.-M.; Wu, C.-C.; Hsieh, P.-W.; Chen, S.-L.; Chang, F.-R.; Hung, W.-C.; Issa, H.H.; Wu, Y.-C. Cytotoxic sesquiterpene lactones from *Pseudelephantopus spicatus*. *J. Nat. Prod.* **2007**, *70*, 1761–1765. [[CrossRef](#)]
22. Girardi, C.; Fabre, N.; Paloque, L.; Ramadani, A.P.; Benoit-Vical, F.; González-Aspajo, G.; Haddad, M.; Rengifo, E.; Jullian, V. Evaluation of antiplasmodial and antileishmanial activities of herbal medicine *Pseudelephantopus spiralis* (Less.) Cronquist and isolated hirsutinolide-type sesquiterpenoids. *J. Ethnopharmacol.* **2015**, *170*, 167–174. [[CrossRef](#)]
23. Usuga, N.d.S.J.; Malafronte, N.; Durango, E.J.O.; Braca, A.; De Tommasi, N. Phytochemical investigation of *Pseudelephantopus spiralis* (Less.) Cronquist. *Phytochem. Lett.* **2016**, *15*, 256–259. [[CrossRef](#)]
24. Odonne, G.; Herbet, G.; Eparvier, V.; Bourdy, G.; Rojas, R.; Sauvain, M.; Stien, D. Antileishmanial sesquiterpene lactones from *Pseudelephantopus spicatus*, a traditional remedy from the *Chayahuita Amerindians* (Peru). Part III. *J. Ethnopharmacol.* **2011**, *137*, 875–879. [[CrossRef](#)] [[PubMed](#)]
25. Ren, Y.; Yu, J.; Kinghorn, A.D. Development of anticancer agents from plant-derived sesquiterpene lactones. *Curr. Med. Chem.* **2016**, *23*, 2397–2420. [[CrossRef](#)] [[PubMed](#)]
26. Quintana, J.; Estévez, F. Recent advances on cytotoxic sesquiterpene lactones. *Curr. Pharm. Des.* **2018**, *24*, 4355–4361. [[CrossRef](#)] [[PubMed](#)]
27. Sheetal, C.; Mishra, P.K. A review on pharmacognocny of bioactive sesquiterpene lactones. *Int. J. Pharmacogn. Phytochem. Res.* **2019**, *11*, 116–121.
28. Mandal, S.K.; Debnath, U.; Kumar, A.; Thomas, S.; Mandal, S.C.; Choudhury, M.D.; Palit, P. Natural sesquiterpene lactones in the prevention and treatment of inflammatory disorders and cancer: A systematic study of this emerging therapeutic approach based on chemical and pharmacological aspect. *Lett. Drug Des. Discov.* **2020**, *17*, 1102–1116. [[CrossRef](#)]
29. Miklossy, G.; Youn, U.J.; Yue, P.; Zhang, M.; Chen, C.-H.; Hilliard, T.S.; Paladino, D.; Li, Y.; Choi, J.; Sarkaria, J.N. Hirsutinolide series inhibit Stat3 activity, alter GCN1, MAP1B, Hsp105, G6PD, vimentin, TrxR1, and importin α -2 expression, and induce antitumor effects against human glioma. *J. Med. Chem.* **2015**, *58*, 7734–7748. [[CrossRef](#)] [[PubMed](#)]
30. Yu, H.; Kortylewski, M.; Pardoll, D. Crosstalk between cancer and immune cells: Role of STAT3 in the tumour microenvironment. *Nat. Rev. Immunol.* **2007**, *7*, 41–51. [[CrossRef](#)]
31. Sellier, H.; Rébillard, A.; Guette, C.; Barré, B.; Coqueret, O. How should we define STAT3 as an oncogene and as a potential target for therapy? *Jak-Stat* **2013**, *2*, e24716. [[CrossRef](#)]
32. Bray, F.; Ferlay, J.; Soerjomataram, I.; Siegel, R.L.; Torre, L.A.; Jemal, A. Global cancer statistics 2018: GLOBOCAN estimates of incidence and mortality worldwide for 36 cancers in 185 countries. *CA Cancer J. Clin.* **2018**, *68*, 394–424. [[CrossRef](#)]

33. INCA. *Estimativa 2020: Incidência de câncer no Brasil*; Instituto Nacional de Câncer José Alencar Gomes da Silva, Ministério da Saúde: Rio de Janeiro, Brazil, 2019; pp. 1–120.
34. De Cicco, P.; Busà, R.; Ercolano, G.; Formisano, C.; Allegra, M.; Tagliatela-Scafati, O.; Ianaro, A. Inhibitory effects of cynaropicrin on human melanoma progression by targeting MAPK, NF- κ B, and Nrf-2 signaling pathways in vitro. *Phytother. Res.* **2021**, *35*, 1432–1442. [[CrossRef](#)]
35. Rozenblat, S.; Grossman, S.; Bergman, M.; Gottlieb, H.; Cohen, Y.; Dovrat, S. Induction of G₂/M arrest and apoptosis by sesquiterpene lactones in human melanoma cell lines. *Biochem. Pharmacol.* **2008**, *75*, 369–382. [[CrossRef](#)]
36. Li, H.; Li, J.; Liu, M.; Xie, R.; Zang, Y.; Li, J.; Aisa, H.A. Guaianolide sesquiterpene lactones from *Achillea millefolium* L. *Phytochemistry* **2021**, *186*, 112733. [[CrossRef](#)]
37. Da Silva, L.A.L.; Sandjo, L.P.; Fratoni, E.; Moon, Y.J.K.; Dalmarco, E.M.; Biavatti, M.W. A single-step isolation by centrifugal partition chromatography of the potential anti-inflammatory glaucolide B from *Lepidaploa chamissonis*. *J. Chromatogr. A* **2019**, *1605*, 1–8. [[CrossRef](#)]
38. Jakupovic, J.; Schmeda-Hirschmann, G.; Schuster, A.; Zdero, C.; Bohlmann, F.; King, R.M.; Robinson, H.; Pickardt, J. Hirsutinolides, glaucolides and sesquiterpene lactone from *Vernonia* species. *Phytochemistry* **1986**, *25*, 145–158. [[CrossRef](#)]
39. Le Roux, C.; Mandrou, S.; Dubac, J. First catalytic C-acylation of enoxysilanes: An efficient route to β -diketones. *J. Org. Chem.* **1996**, *61*, 3885–3887. [[CrossRef](#)]
40. Salvador, J.A.; Silvestre, S.M.; Pinto, R. Bismuth (III) reagents in steroid and terpene chemistry. *Molecules* **2011**, *16*, 2884–2913. [[CrossRef](#)]
41. Rodríguez-Hahn, L.; Cárdenas, J.; Maldonado, E.; Ortega, A.; Martínez, M.; Soriano Garcia, M.; Toscano, A. Transannular cyclization of glaucolide A. *J. Org. Chem.* **1988**, *53*, 2965–2968. [[CrossRef](#)]
42. Hua, R. Recent advances in bismuth-catalyzed organic synthesis. *Curr. Org. Synth.* **2008**, *5*, 1–27. [[CrossRef](#)]
43. Salvador, J.A.R.; Pinto, R.; Silvestre, S.M. Recent advances of bismuth (III) salts in organic chemistry: Application to the synthesis of aliphatics, alicyclics, aromatics, amino acids and peptides, terpenes and steroids of pharmaceutical interest. *Mini Rev. Org. Chem.* **2009**, *6*, 241–274. [[CrossRef](#)]
44. Salvador, J.A.; Pinto, R.; Silvestre, S.M. Recent advances of bismuth (III) salts in organic chemistry: Application to the synthesis of heterocycles of pharmaceutical interest. *Curr. Org. Synth.* **2009**, *6*, 426–470. [[CrossRef](#)]
45. Ondet, P.; Lemièrre, G.; Duñach, E. Cyclisations catalysed by bismuth (III) triflate. *Eur. J. Org. Chem.* **2017**, *2017*, 761–780. [[CrossRef](#)]
46. Catalán, C.A.N.; De Iglesias, D.I.A.; Kavka, J.; Sosa, V.E.; Herz, W. Glaucolides and related sesquiterpene lactones from *Vernonia chamaedrys*. *Phytochemistry* **1988**, *27*, 197–202. [[CrossRef](#)]
47. Mandai, H.; Fujii, K.; Yasuhara, H.; Abe, K.; Mitsudo, K.; Korenaga, T.; Suga, S. Enantioselective acyl transfer catalysis by a combination of common catalytic motifs and electrostatic interactions. *Nat. Commun.* **2016**, *7*, 11297. [[CrossRef](#)] [[PubMed](#)]
48. Xu, S.; Held, I.; Kempf, B.; Mayr, H.; Steglich, W.; Zipse, H. The DMAP-catalyzed acetylation of alcohols—A mechanistic study (DMAP= 4-(dimethylamino)pyridine). *Chem. Eur. J.* **2005**, *11*, 4751–4757. [[CrossRef](#)]
49. Fischer, C.B.; Xu, S.; Zipse, H. Steric effects in the uncatalyzed and DMAP-catalyzed acylation of alcohols—Quantifying the window of opportunity in kinetic resolution experiments. *Chem. Eur. J.* **2006**, *12*, 5779–5784. [[CrossRef](#)]
50. Ouellette, R.J.; Rawn, J.D. Haloalkanes and alcohols: Introduction to nucleophilic substitution and elimination reactions. In *Organic Chemistry: Structure, Mechanism, and Synthesis*; Ouellette, R.J., Rawn, J.D., Eds.; Elsevier: San Diego, CA, USA, 2014; pp. 287–331.
51. Bohlmann, F.; Zdero, C.; King, R.M.; Robinson, H. Neue sesquiterpenlactone aus *Stokesia laevis*. *Phytochemistry* **1979**, *18*, 987–989. [[CrossRef](#)]
52. Bohlmann, F.; Mahanta, P.K.; Dutta, L.N. Weitere hirsutinolide aus *Vernonia*-arten. *Phytochemistry* **1979**, *18*, 289–291. [[CrossRef](#)]
53. Aliarab, A.; Abroon, S.; Rasmi, Y.; Aziz, S.G.-G. Application of sesquiterpene lactone: A new promising way for cancer therapy based on anticancer activity. *Biomed. Pharmacother.* **2018**, *106*, 239–246.
54. Serasanambati, M.; Chilakapati, S.R. Function of nuclear factor kappa B (NF- κ B) in human diseases—A review. *South Indian J. Biol. Sci.* **2016**, *2*, 368–387. [[CrossRef](#)]
55. D'Anneo, A.; Carlisi, D.; Lauricella, M.; Emanuele, S.; Di Fiore, R.; Vento, R.; Tesoriere, G. Parthenolide induces caspase-independent and AIF-mediated cell death in human osteosarcoma and melanoma cells. *J. Cell. Physiol.* **2013**, *228*, 952–967. [[CrossRef](#)] [[PubMed](#)]
56. Maldonado, E.; Svensson, D.; Oredsson, S.; Sterner, O. Cytotoxic sesquiterpene lactones from *Kauna lasiophthalma* Griseb. *Sci. Pharm.* **2014**, *82*, 147–160. [[CrossRef](#)] [[PubMed](#)]
57. Chen, L.; Zhang, J.-P.; Liu, X.; Tang, J.-J.; Xiang, P.; Ma, X.-M. Semisynthesis, an anti-inflammatory effect of derivatives of 1 β -hydroxy alantolactone from *Inula britannica*. *Molecules* **2017**, *22*, 1835. [[CrossRef](#)]
58. Nakagawa-Goto, K.; Chen, J.-Y.; Cheng, Y.-T.; Lee, W.-L.; Takeya, M.; Saito, Y.; Lee, K.-H.; Shyur, L.-F. Novel sesquiterpene lactone analogues as potent anti-breast cancer agents. *Mol. Oncol.* **2016**, *10*, 921–937. [[CrossRef](#)]
59. Saroglou, V.; Karioti, A.; Demetzos, C.; Dimas, K.; Skaltsa, H. Sesquiterpene Lactones from *Centaurea spinosa* and their antibacterial and cytotoxic activities. *J. Nat. Prod.* **2005**, *68*, 1404–1407. [[CrossRef](#)]

60. Da Silva, L.A.L.; Sandjo, L.P.; Misturini, A.; Caramori, G.F.; Biavatti, M.W. ESI-QToF-MS characterization of hirsutinolide and glaucolide sesquiterpene lactones: Fragmentation mechanisms and differentiation based on Na⁺/H⁺ adducts interactions in complex mixture. *J. Mass Spectrom.* **2019**, *54*, 915–932. [[CrossRef](#)] [[PubMed](#)]
61. Lu, Y.-C.; Yeh, W.-C.; Ohashi, P.S. LPS/TLR4 signal transduction pathway. *Cytokine* **2008**, *42*, 145–151. [[CrossRef](#)]
62. Wang, N.; Liang, H.; Zen, K. Molecular mechanisms that influence the macrophage M1–M2 polarization balance. *Front. Immunol.* **2014**, *5*, 614. [[CrossRef](#)]
63. Dirsch, V.M.; Stuppner, H.; Ellmerer-Müller, E.P.; Vollmar, A.M. Structural requirements of sesquiterpene lactones to inhibit LPS-induced nitric oxide synthesis in RAW 264.7 macrophages. *Bioorg. Med. Chem.* **2000**, *8*, 2747–2753. [[CrossRef](#)]
64. Han, I.-H.; Song, H.-O.; Ryu, J.-S. IL-6 produced by prostate epithelial cells stimulated with *Trichomonas vaginalis* promotes proliferation of prostate cancer cells by inducing M2 polarization of THP-1-derived macrophages. *PLOS Negl. Trop. Dis.* **2020**, *14*, e0008126. [[CrossRef](#)] [[PubMed](#)]
65. Wagner, H.; Bladt, S. *Plant Drug Analysis: A Thin Layer Chromatography Atlas*, 2nd ed.; Springer: London, UK, 2001.
66. ChemAxon Marvin 19.1.11.0. Available online: <https://www.chemaxon.com> (accessed on 27 January 2016).
67. ChemAxon Standardizer JChem 16.1.11.0. Available online: <https://www.chemaxon.com> (accessed on 27 January 2016).
68. Imre, G.; Veress, G.; Volford, A.; Farkas, Ö. Molecules from the Minkowski space: An Approach to Building 3D Molecular structures. *J. Mol. Struct. THEOCHEM* **2003**, *666*, 51–59. [[CrossRef](#)]
69. Spartan. Model Homepage for Windows. Available online: http://www.wavefun.com/products/windows/SpartanModel/win_model.html (accessed on 27 April 2013).
70. Halgren, T.A. Merck molecular force field. I. Basis, form, scope, parameterization, and performance of MMFF94. *J. Comput. Chem.* **1996**, *17*, 490–519. [[CrossRef](#)]
71. Stewart, J.J.P. Optimization of parameters for semiempirical methods V: Modification of NDDO approximations and application to 70 elements. *J. Mol. Model.* **2007**, *13*, 1173–1213. [[CrossRef](#)] [[PubMed](#)]
72. Metropolis, N.; Ulam, S. The Monte Carlo method. *J. Am. Stat. Assoc.* **1949**, *44*, 335–341. [[CrossRef](#)]
73. Becke, A.D. Density-functional exchange-energy approximation with correct asymptotic behavior. *Phys. Rev. A* **1988**, *38*, 3098–3100. [[CrossRef](#)]
74. Lin, C.Y.; George, M.W.; Gill, P.M.W. EDF2: A density functional for predicting molecular vibrational frequencies. *Aust. J. Chem.* **2004**, *57*, 365–370. [[CrossRef](#)]
75. Mosmann, T. Rapid colorimetric assay for cellular growth and survival: Application to proliferation and cytotoxicity assays. *J. Immunol. Methods.* **1983**, *65*, 55–63. [[CrossRef](#)]
76. Lavogina, D.; Lust, H.; Tahk, M.-J.; Laasfeld, T.; Vellama, H.; Nasirova, N.; Vardja, M.; Eskla, K.-L.; Salumets, A.; Rinke, A. Revisiting the resazurin-based sensing of cellular viability: Widening the application horizon. *Biosensors* **2022**, *12*, 196. [[CrossRef](#)]
77. Herath, H.M.T.; Takano-Ishikawa, Y.; Yamaki, K. Inhibitory effect of some flavonoids on tumor necrosis factor- α production in lipopolysaccharide-stimulated mouse macrophage cell line J774. 1. *J. Med. Food* **2003**, *6*, 365–370. [[CrossRef](#)] [[PubMed](#)]
78. Griess, P. Bemerkungen zu der Abhandlung der HH. Weselky und Benedikt ueber einege Azoverbindungen. *Ber. Dtsch. Chem. Ges.* **1879**, *12*, 426–428. [[CrossRef](#)]

Disclaimer/Publisher’s Note: The statements, opinions and data contained in all publications are solely those of the individual author(s) and contributor(s) and not of MDPI and/or the editor(s). MDPI and/or the editor(s) disclaim responsibility for any injury to people or property resulting from any ideas, methods, instructions or products referred to in the content.